NTNU

Norwegian University of
Science and Technology

Gas Turbine Operation

Drift av Gassturbiner

Edvard Aamodt

Natural Gas Technology
Submission date: July 2018
Supervisor: Lars Eirik Bakken, EPT
Co-supervisor: Stian Madsen, EPT

Norwegian University of Science and Technology
Department of Energy and Process Engineering

Project description

NTNU
Norwegian University
of Science and Technology

Department of Energy
and Process Engineering

EPT-M-2018-01

MASTER THESIS

for

student Edvard Aamodt

Spring 2018

Gas Turbine Operation
Drift av gassturbiner

Background and objective

Increased focus on energy efficiency and reduced emissions to air from gas turbine power production applies on both design and operation. Experience demonstrate a large incentive to analyse and understand the gas turbine response to different operating modes.

The main objective is to analyse and document different anti-icing modes and how these affects the gas turbine performance and emissions. The work should be based on "state-of-the-art" technology and include utilization of compressor bleed air.

The following tasks are to be considered:

1. Literature review to document different anti-icing technologies and their functionality.
2. Perform analyses and document how the different technologies affect the gas turbine performance and emissions.
3. Establish procedure to correct the compressor and gas turbine efficiency when utilising compressor bleed air for anti-icing. Use of dimensional parameters may be beneficial.

-- " --

Within 14 days of receiving the written text on the master thesis, the candidate shall submit a research plan for his project to the department.

When the thesis is evaluated, emphasis is put on processing of the results, and that they are presented in tabular and/or graphic form in a clear manner, and that they are analyzed carefully.

The thesis should be formulated as a research report with summary both in English and Norwegian, conclusion, literature references, table of contents etc. During the preparation of the text, the candidate should make an effort to produce a well-structured and easily readable report. In order to ease the evaluation of the thesis, it is important that the cross-references are correct. In the making of the report, strong emphasis should be placed on both a thorough discussion of the results and an orderly presentation.

The candidate is requested to initiate and keep close contact with his/her academic supervisor(s) throughout the working period. The candidate must follow the rules and regulations of NTNU as well as passive directions given by the Department of Energy and Process Engineering.

Risk assessment of the candidate's work shall be carried out according to the department's procedures. The risk assessment must be documented and included as part of the final report. Events related to the candidate's work adversely affecting the health, safety or security, must be documented and included as part of the final report. If the documentation on risk assessment represents a large number of pages, the full version is to be submitted electronically to the supervisor and an excerpt is included in the report.

Pursuant to "Regulations concerning the supplementary provisions to the technology study program/Master of Science" at NTNU §20, the Department reserves the permission to utilize all the results and data for teaching and research purposes as well as in future publications.

The final report is to be submitted digitally in DAIM. An executive summary of the thesis including title, student's name, supervisor's name, year, department name, and NTNU's logo and name, shall be submitted to the department as a separate pdf file. Based on an agreement with the supervisor, the final report and other material and documents may be given to the supervisor in digital format.

☐ Work to be done in lab (Water power lab, Fluids engineering lab, Thermal engineering lab)
☐ Field work

Department of Energy and Process Engineering, 19. February 2018

L E Bakken
Academic Supervisor

Research Advisor:
S. Madsen

Acknowledgements

This master's project is the final work for the degree in Master of Science in Natural Gas Technology at the Norwegian University of Science and Technology, with specialisation in Energy, Process and Flow Engineering. The work is supposed to be a solitary and independent work but is as everything else in life done with the help of others.

I would like to sincerely thank my supervisor Professor Lars Eirik Bakken for his invaluable help and teachings in the world of gas turbines, and contributions and moral support through this whole process. Thanks also to co-supervisor Stian-Mikal Madsen for help and for providing valuable data to base this work on.

Most importantly I want to thank my dear family and friends at home for always supporting me whenever the going got tough. Along the way new friends have arrived and to the people of UKA I will never forget you, we made history! Also, my study pals John, Inez, Ali, Raphael, Niklas, Steffen and Nadim and my sister Solveig, next round is upon me!

And finally Tuva, the support you and your family have given is without doubt the biggest contributor to finishing this thesis. I would not have made it down the road with one head light.

When I look back
I see the landscapes
That I have walked through
But it is different
All the great trees are gone
It seems there are
Remnants of them
But it is the afterglow
Inside of you
Of all those you met
Who meant something in your life – Olav V Rex, 1977

This thesis is dedicated to my dear grandmother Else Ågot Kjøstvedt (1923-2018). In an engineering life full of mysterious and puzzling variables to chase, it is far too easy to forget the great constants, you being the greatest of them all.

Trondheim, 15.07.2018

Abstract

Important power and mechanical drive demands offshore are met by utilizing gas turbines. The safe and reliable operation of these fine-tuned thermo machines are of key importance to maintain platform operation. Problems related to challenging weather conditions and especially ice, are of real concern to engineers. Icing both precipitate and condensate are found to occur in gas turbines, and are only dealt with utilizing anti-icing measures, such as anti-icing systems and filters.

Anti-icing systems mostly used today comes with considerable costs to gas turbine efficiency, and prompts higher emissions to air. An extensive literature study of state-of-the-art anti-icing technologies have been conducted in this thesis. The operational impact the systems have on the gas turbine performance has been mapped. Waste heat recovery method of prevention has been documented to have a relatively small impact on operation. Analysing operational data from two LM2500PE gas turbines offshore confirms this notion. In the analysis the deviation in important performance parameters such as GG speed (N_1), and Pressure Ratio (PR), is more prominent in the gas turbine utilizing hot bleed extraction. The mass flow extraction is believed to be the cause of these deviations in performance parameters. The waste heat recovery system utilizes exhaust gas instead of compressor discharge air, as heat medium, which makes it the preferred system to install.

The hot bleed anti-icing system is documented to impact both compressor and gas turbine efficiencies. The deviations in polytropic compressor and thermal efficiency needs correcting. Correcting these efficiency trends will make detecting and diagnosing malfunctions easier. Polytropic efficiency was found to deviate due to altered N_{1c} and PR_c. Thermal efficiency deviated because compressor delivery temperature (T_{3c}) was altered. A correction procedure was suggested, and it proved promising as polytropic and thermal deviation was reduced from 3% to -1% and 2.4% to 0.4% for baseload, respectively. The part load running machines were corrected from 5.5% to 1% and 4.2% to 1.8% respectively.

Abstract in Norwegian

Viktige krav til strøm- og mekanisk drivkraft i offshoreindustrien blir møtt ved bruk av gassturbiner. Sikker og pålitelig drift av disse delikate termomaskinene er viktig for hele plattformens daglige drift. Problemer angående ekstreme værforhold og spesielt isdannelse er store bekymringer for ingeniører. Ising fra kondensdannelse eller vann i forskjellige faser kan oppstå i gassturbinene, og hindres ved bruk av anti-is metoder som for eksempel egne anti-issystemer og innløpsfiltre.

De anti-issystemene som brukes i dag kommer med betraktelige kostnader for gassturbinens effektivitet, og promoterer høyere utslipp til luften. En grundig litteraturstudie for relevante anti-is teknologier har blitt gjennomført i denne oppgaven. Innvirkningene disse systemene har på ytelsen til maskinene har blitt kartlagt. Waste heat recovery-systemets metode for isforebygging er blitt dokumentert i flere kilder som det minst innvirkende systemet på driften av gassturbiner. Forfatterens analyse av driftdata fra to LM2500PE bekrefter denne innstillingen. I analysen ble avvik i viktige ytelsesparametre som GG Fart (N_{1c}) og Trykkratio (PR_c) tydeligere når gassturbinen brukte hot bleed extraction-systemet. At dette systemet drar varm luft fra kompressorens utløp er grunnen til dette relativt store avviket i ytelsesparametre. Waste heat recovery-systemet bruker eksosgass som varmekilde noe som gjør det til et fortrukket system for isforebygging.

Hot bleed-systemet er dokumentert å ha innvirkning på både polytropisk kompressor- og termisk virkningsgrad. Disse avvikene i ytelsestrender trenger å korrigeres. En korrigering av disse trendene vil gjøre arbeidet med oppdagelse og diagnosering av feil på maskinene lettere. Polytropisk virkningsgrad avviket fra trenden pga. skiftet i N_{1c} og PR_c, og termisk virkninggrad avviket pga. temperaturen fra kompressoren (T_{3c}) endret seg. En korreksjonsprosedyre er foreslått og ser lovende ut når polytropisk og termisk avvik er redusert fra 3% til -1% og 2,4% til 0,4% for vanlig drift, respektivt. Ved lavere turtall, også kalt part load, ble korrigeringen 5,5% til 1% og 4,2 % til 1,8% respektivt.

Contents

List of figures

List of tables

Nomenclature

Symbols

P	Pressure	$[bar]$
T	Temperature	$[K]$
N_1	Rotational Speed GG	$[rpm]$
N_2	Rotational Speed PT	$[rpm]$
h	Enthalpy	$[kJ/kg]$
s	Entropy	$[kJ/kg \cdot K]$
P	Power	$[J/s]$
X/Y	Compressibility Function	-
m	Polytropic Temperature Exponent	-
n	Polytropic Volume Exponent	-
R	Gas Constant	$[J/mol \cdot K]$
Z	Compressibility Factor	-
a	Molecule Factor	-
b	Molecule Factor	-
W	Work	$[J]$
C_p	Heat Capacity at Constant Pressure	-
C_v	Heat Capacity at Constant Pressure	-
K	Correction Factor	-
Y	Parameter of Interest	-
k	Heat Capacity Ratio	

Table 1: Explanation of symbols

Greek Symbols

η	Efficiency	$[\%]$
n	Polytropic Exponent	-
δ	Mach Number Correction Factor	-
Θ	Mach Number Correction Factor	-
ρ	Density	kg/m^3
ω	Acentric Factor	-
Δ	Change in Parameter	-

Table 2:Explanation of Greek symbols.

Subscripts

0	Ambient/initial
2	Compressor Inlet
3	Compressor Discharge
5.4	HPT discharge
c	Corrected/Critical
ref	Reference
s	Isentropic
p	Polytropic
t	Thermal

Table 3:Explanation of subscripts.

Abbreviations

GG	Gas Generator
HPT	High Pressure Ratio
PT	Power/Free Turbine
GE	General Electric
VIGV	Variable Inlet Guide Vane
CFF	Compressor Front Frame
CRF	Compressor Rear Frame
TMF	Turbine Mid Frame
TRF	Turbine rear Frame
PR	Pressure Ratio
TIT	Turbine Inlet Temperature
EGT	Exhaust Gas Temperature
ISO	International Standard Organization
EOS	Equation of State
NOK	Norwegian Kroner
BEP	Best Efficiency Point
SRK	Soave-Redlich-Kwong
SAC	Single Annular Combustor
DLE	Dry Low Emission

Table 4:Explanation of abbreviations.

1. Introduction

This introduction provides the background for the work in this thesis, describes why this topic was chosen. The scope of the work is then discussed and last an explanation to the structure of the thesis is provided.

1.1 Background

Most of the power consumption processes and equipment drivers on offshore processing plants are today run by gas turbines. For these finetuned internal combustion engines the intake air for the compressor is a key factor for the engines' overall performance. Critical problems for the reliable and efficient supply of energy are gas turbine fouling and ice and vapour ingestion. The latter inducing ice formation which builds up on the inlet components causing a pressure drop across the inlet air reducing the performance. In extreme cases the ice can cause foreign object damage and compressor surge.

In the harsh conditions offshore, cold and humidity are particularly common challenges, and anti-icing systems and other preventive methods are numerous and have been in service for a long time. However, using these technologies does not come without significant side effects, resulting in performance loss, and optimizing these methods can therefore grant sizable recovery of performance.

Therefore, this work will present different types of anti-icing technology through literature review, and analyse the effects these preventive measures have on the operation of the gas turbine. The analysis will broaden the knowledge base of gas turbine behaviour and performance trends. Signature patterns in performance trends can then be recognized, and operators can then easily avoid making false alarms due to suspicion of a malfunction.

During hot bleed anti-icing activation the efficiency trends of the gas turbine are expected to deviate, making an anomaly in performance parameters. Correction procedures to normalize these anomalies are wanted by the industry, as they can ensure stabile operation of the engines. Correcting these parameters will also make it easier to uncover malfunctions hidden within the measured parameters.

1.2 Scope of work

The work covers state-of-the-art ice technologies, and presents how these technologies work and affect the operation of gas turbines situated in cold environments.

The two most used anti-ice technologies are the hot bleed and waste heat recovery systems. To limit the scope of this thesis these two technologies are chosen to be analysed. Two General Electric LM2500PE gas turbines situated offshore are analysed through operational data, before and after anti ice activation. These engines consist of a generator drive referred to as engine A, and a mechanical drive referred to as engine B. Engine A comes equipped with the hot bleed air system and B with the waste heat recovery system.

Efficiencies are expected to vary greatly with the warmer inlet air when anti-ice is activated, this is accounted for in operation. Deviations caused by mass flow extraction however must be examined further. The extraction of mass flow is unique to hot bleed systems, and a procedure correcting for the extraction of mass flow is therefore proposed to make engine operation and diagnostic easier and more reliable.

1.3 Thesis structure

Chapter 1 consist of an introduction to the master thesis, clarifying the scope of the work and how the thesis is structured.

Chapter 2 introduces gas turbine theory, how the machine components work and operate, and how they are analysed.

Chapter 3 gives a brief introduction to the ice formation experienced by the gas turbines and why anti-ice technologies are important for steady operation.

Chapter 4 presents several anti-ice technologies and supplementing equipment for gas turbine intakes, and how these are influencing the operation.

Chapter 5 contains the analysis of the two different anti-ice technologies deployed on the gas turbines offshore.

Chapter 6 suggests a procedure of correcting the mass flow extraction done by the hot bleed anti-ice technology.

Chapter 7 includes a summary of the work and a conclusion.

Chapter 8 suggests work for further investigation and ideas on what engineers can take into consideration.

2. Gas turbine theory

This chapter introduces gas turbine theory, engine components and their characteristics. It will also serve as the foundation from which calculations and analyses are done throughout the thesis. This chapter builds on previous project-work done by the author [2], but with considerable changes and improvements.

2.1 General operation

Gas turbines are used on offshore platform plants both for power generation and as drivers for mechanical equipment such as compressors. They follow the thermodynamic principles of the Brayton cycle. This cycle involves compression of the gas, subsequent heating of the gas by burning of fuel, followed by an expansion of the hot compressed gas. The first three steps are referred to as a gas generator (GG) comprised of a compressor, a combustion chamber, and a high-pressure turbine (HPT). Utilizing the compressed, heated gas for expansion, the HPT drives the compressor, and a power turbine (PT) is using the remaining energy in the gas for shaft power output. More on thermodynamic principles in gas turbines, and how the machines work is extensively covered in Gas Turbine Theory in Saravanamuttoo [3].

The following sections describe the evaluated gas turbines.

2.2 Evaluated engines

This thesis will focus on the LM2500PE gas turbines from General Electric (GE) situated on platforms offshore. These gas turbines generate power to the platform as well as the nearby platforms and in addition another set of the same gas turbine is used for operating the compressor drives on the field. Throughout the thesis the power generating gas turbine is referred to as engine A and the compressor drive gas turbine referred to as engine B.

LM2500PE is a twin-shaft aeroderivative gas turbine consisting of a gas generator and a power turbine, depicted in Figure 1. The twin-shaft arrangement provides considerable flexibility when driving a variable speed load such as the compressor drive that engine B is connected to. Although analysis in this thesis relies on results from a specific pair of engines, its relevance spans for several engine types of similar configuration, experiencing the same conditions.

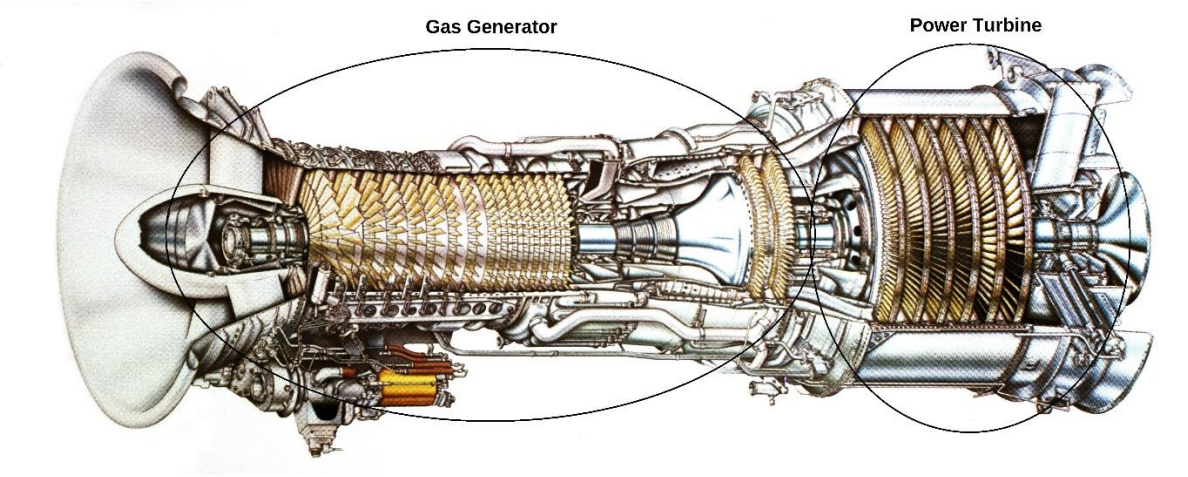

Figure 1: LM2500 cutaway with indication of gas generator and power turbine [4].

2.3 The gas turbine components

2.3.1 Compressor

The axial compressor section of the LM2500PE consists of 16 stages. The first stage is made up of a row of rotor blades followed by a row of stator blades. The rotor blades are accelerating the working fluid which transfers its kinetic energy on to the rotor blades, converting it into static pressure [3]. Axial compressors are generally chosen because they have higher compression ratio and efficiency, but also because they swallow more air for their size. The first six stages of the LM2500 compressor are variable inlet guide vanes (VIGV) to vary the entering flow angle, and through the stages a compression ratio of up to 20:1 is generated [4].

The compressor section is the first to be exposed to the ambient air as it flows through the intake. Therefore, analysis of this section is of prime importance when understanding how the gas turbine reacts to changes e.g. varying inlet conditions, particle contamination and ice ingestion. Inlet pressure and temperatures subscripted 2 are measured after the bellmouth in the compressor front frame (CFF), see Figure 3, so all inlet conditions are accounted for. The respective discharge conditions subscripted 3 are monitored in the compressor rear frame (CRF). P_{s3} are measured in static pressure conditions but will be referred to as P_3 for the sake of simplicity.

Often the compressor can get degraded because of both recoverable and non-recoverable deterioration, reducing the performance. As the names suggest, recoverable deterioration covers

all deposits and fouling that can be manually or automatically removed and the non-recoverable entail erosion, corrosion etc. that demand operational shut-down and replacing of engine parts.

Figure 2: Indications of blade and vane deterioration due to sand and water ingestion.

2.3.2 Combustor section

After the working fluid is compressed it is sent to the annular combustion chamber. In this chamber there are 30 nozzles for gas fuel injection which is mixed with air and thereafter burned [4]. The exhaust gas comprising of combustion-deposits and -gases and excessive air is sent to the high-pressure turbine (HPT) at a temperature of approximately 1450 °C.

Combustors in the LM2500 are of the single annular combustor type (SAC). This technology uses premixing and often water ingestion to keep the CO_2 and NO_x emissions down. Although the combustors employ advanced technology to reduce emissions, they must obey the control system, described in detail later, making them burn more fuel, increasing emissions and exhaust gas temperatures.

2.3.3 High pressure turbine

The high-pressure axial turbine (HPT) consists of two stages and delivers shaft power to the compressor and accessory gearbox. The high energy combustion gas and excess air flows through the stator and rotor blades of the turbine, producing rotational energy, which is transferred to the compressor as they both are attached to the same shaft.

Analysing turbine operation and performance is important, but can be more complicated than its compressing counterpart. The expansion process is highly dependent on the operations prior, just explained. Turbine inlet temperatures (TIT) and pressures result in higher turbine performance, but are not given in the analysis data. Temperature $T_{5.4}$ or exhaust gas temperature (EGT) are measured in the turbine mid frame (TMF) after the HPT, see Figure 3. An increase in $T_{5.4}$ is generally linked to higher temperatures from the combustion chamber due to higher fuel flow.

2.3.4 Power turbine

This last section of the gas turbine is a six-stage axial turbine which utilizes the left-over pressure and temperature from the HPT to create shaft power output. It is not mechanically connected to the other components (therefore also called free turbine), but rather rotates on its own shaft at a different speed subscripted as N_2. As mentioned before this shaft power is used for driving a generator or a process compressor drive.

Due to being pneumatically coupled to the GG, this turbine can handle varying load from the power shaft experienced when driving operational equipment, but the matching of the GG to the PT is complicated. The power turbine must ingest the same mass flow of air as the GG and deal with a pressure ratio also fixed by the GG. There is only one point on the constant speed line, in the compressor characteristic, where this equilibrium line can cross, and this must be found by iteration.

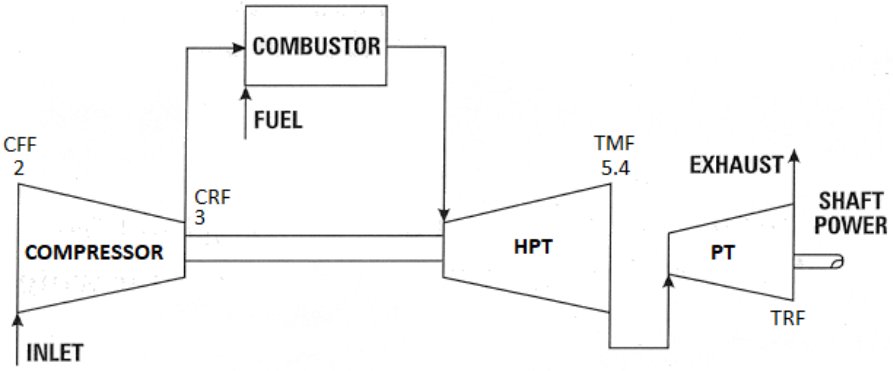

Figure 3: Derived schematic of a gas turbine with Gas Generator and Power Turbine [3].

2.3.5 Control systems

The function of the control system is regulating the performance of the gas turbine and thus avoiding critical operational situations. The system must ensure that the gas generator (GG) speed (N_1), exhaust gas temperature (EGT) [$T_{5.4}$] and the above-mentioned compressor surge are held within limits. Exceeding these limits will damage components and lead to emissions in the exhaust beyond legal limits. Fuel consumption, bleed valves [5] and, in this study, VIGV's are examples of measures that ensures steady operation of the gas turbine at any ambient condition or operating mode.

Knowledge regarding control systems are particularly valuable when anti-ice technology is activated because of the change in inlet conditions. The consequences of these changes for the

operational parameters inside the gas turbine will be discussed in Chapter 5. Note that the control system will respond differently depending on configuration of the engines.

2.4 Gas turbine analysis

This section introduces gas turbine component characteristics that are important when analysing the effects of different anti-icing technology later in this thesis. The focus is on compressors because most of the analysed data relates to compressor operation. It is possible to estimate successive impacts on further downstream components, but existing data is limited.

2.4.1 Analytical presentation

In a gas turbine engine, the match between the compressor and the turbine defines the operating point. These points are in most essential respects a set of operating parameters where equilibrium and unison exist between the compressor and the turbine, including pressures, temperatures and flows.

When evaluating a compressor, a map can and will be utilized in this thesis. This is a diagram created to display the key characteristics of the compressor. It is uniquely generated to every gas turbine produced. The machine must be driven by an external drive and go through extensive testing to have its map created. Unfortunately, manufacturers seldom give them to the operator.

The map in Figure 4 is a generated characteristic for the LM2500 gas turbine, but the parameter lines are not specified to the evaluated compressors in this study. Therefore, generalized maps will be utilized. The compressor pressure ratio is plotted against the corrected mass flow, but it also contains constant speed, efficiency, and surge lines. A compressor following a constant speed line will, with reduced or increased mass flow, deviate from the best efficiency operating point which follows the equilibrium line [3].

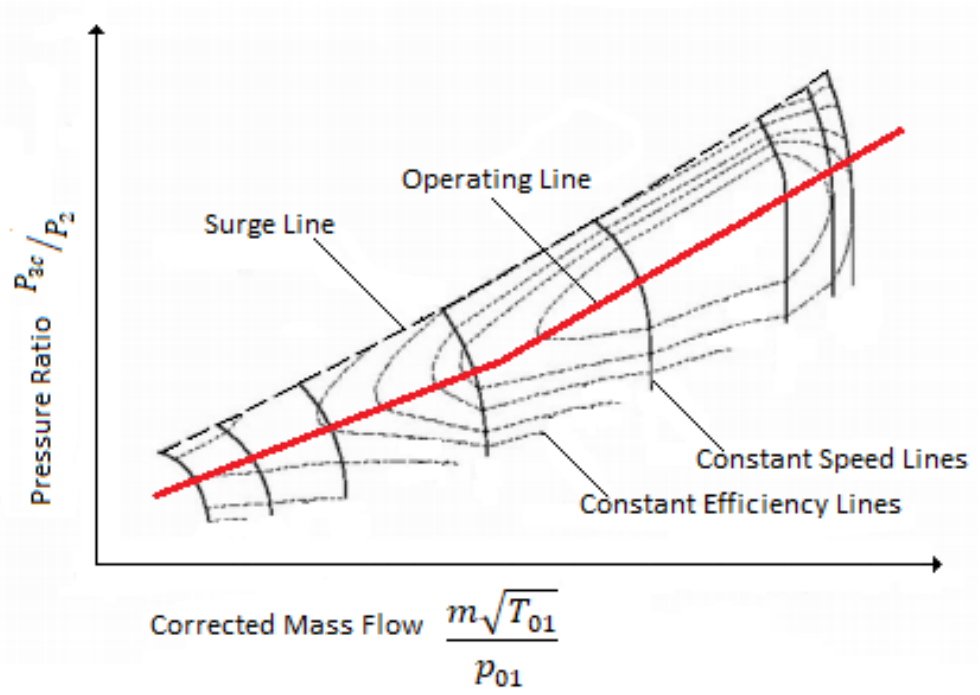

Figure 4: A GE LM2500 compressor map, derived from Dahl [6].

Turbine maps are often given to describe the turbines in the engine and can be generated for both the HPT and the TP. Characteristics of turbines in maps of this sort are also given in corrected mass flow as a function of pressure ratio, with constant speed lines, see Figure 5.

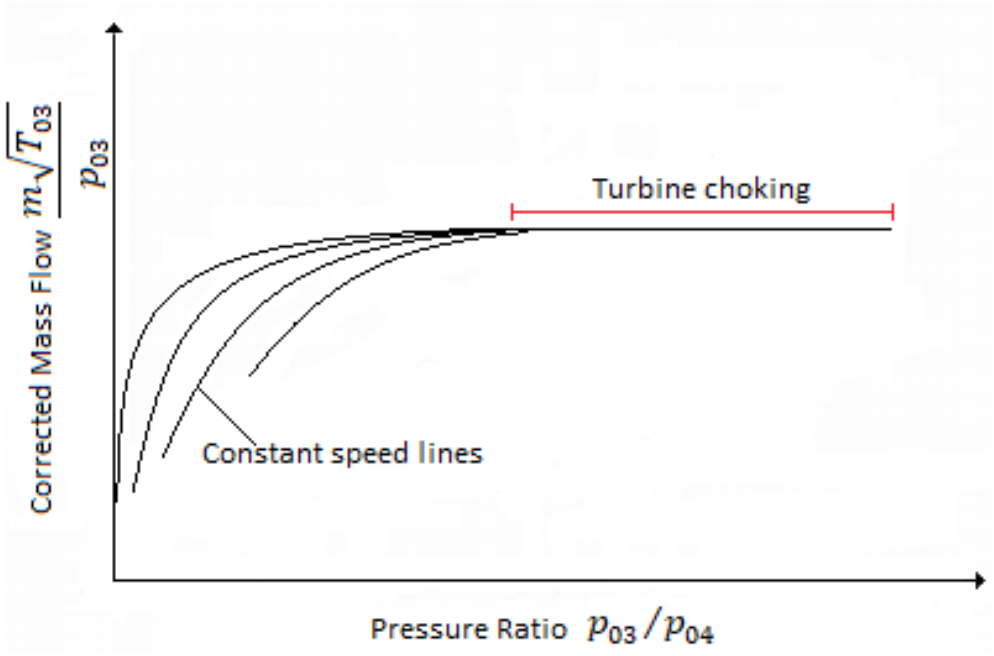

Figure 5: Generalized turbine performance map derived from Saravanamuttoo [3].

As the map suggests the increasing, and maximum, value of mass flow is reached at a pressure ratio that produces choking conditions somewhere in the turbine. Usually this happens in the

nozzle throat, but it can happen elsewhere as well. The constant speed lines all merge into a single horizontal line, and normally both pressure ratio and mass flow will fall when rotational speed decreases.

2.4.2 Flow path analysis

For accurate compression and expansion calculations, both isentropic and polytropic flow path analysis can be utilized. As will be explained later it is preferred that high-pressure analyses are given with the polytropic approach. Figure 6 illustrates the compression process, but it is important to emphasize that the expansion process follows the same fundamental thermodynamic relationships.

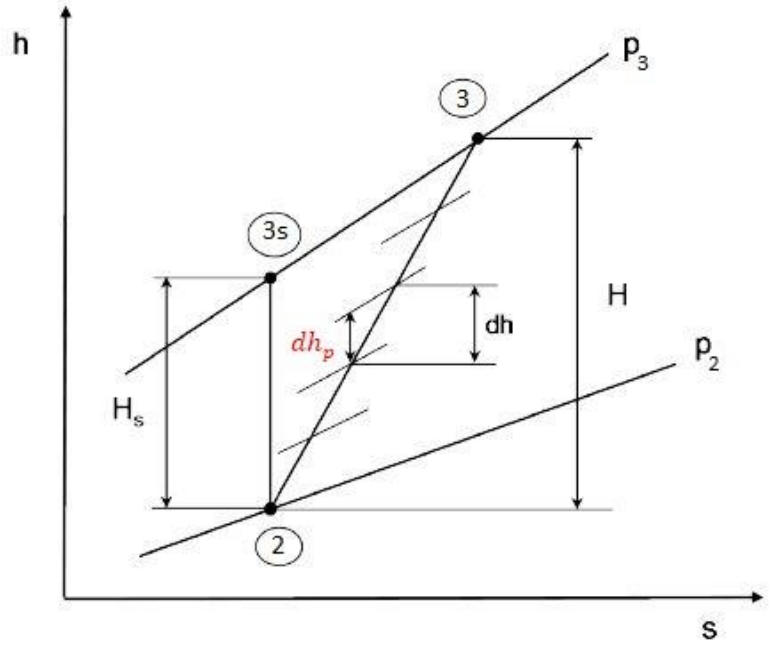

Figure 6: Enthalpy-entropy diagram of a compression process.

In the enthalpy-entropy diagram the isentropic (2 to 3s), polytropic (stepwise 2 to 3) and actual (2 to 3 vertical) process is displayed. The polytropic stepwise analysis is the infinitesimal series dh_p shown in red. The isentropic and actual head, H_s and H respectively, is given in Figure 6 along with the polytropic H_p being the sum of all these steps. Polytropic efficiency will then be as Equation 1 and isentropic in the same fashion.

$$\eta_p = \frac{H_p}{H} \tag{1}$$

Equation 2 displays the polytropic relationship between pressure and temperature where *n* is the polytropic exponent:

$$\frac{T_2}{T_1} = \left(\frac{p_2}{p_1}\right)^{\frac{n-1}{n\eta_p}} \quad (2)$$

As the pressure ratios are relatively high in the analyses done in this thesis, the isobars in Figure 6 will diverge significantly. This indicates that the polytropic efficiency, which takes this divergence into account, is best suited as the preferred efficiency indicator.

To indicate overall efficiency of a gas turbine the term "thermal efficiency" is often used in the literature. This term must include a form of work output versus heat supplied and is strongly connected to specific fuel consumption (SFC) and mass flow. These two parameters are not available in the data given for this thesis. A theoretical equation utilizing the polytropic relationship between pressure and temperature can indicate theoretical thermal efficiency trends and assumptions can be made. PR represents pressure ratio between combustor pressure and ambient pressure.

$$\eta_t = 1 - \left(\frac{1}{PR}\right)^{\frac{n-1}{n\eta_p}} \quad (3)$$

2.4.3 Correction of operational parameters

The conditions of the medium flowing through the gas turbine are important when analysing the performance of turbomachines such as the gas turbine. These performance parameters vary with the inlet conditions and to be comparable for performance analysis they must be corrected by referring them to the certain reference values . Many references cover how to correct these parameters by referring them to typical "day conditions". A very good and respected presentation is done by Valponi [1], where the full theoretical background for Mach number similarities parameters are presented.

The International Standard Organisation (ISO) 3214 describes certain "standard day" conditions which can be utilized in given correction parameter formulas. These conditions centre on inlet temperature of 288.15 K given as θ, a pressure of 101.325 kPa given as δ and 60 % relative humidity in Equation 4, where X is the parameter to be corrected:

$$X_c = \frac{X}{\theta^a \cdot \delta^b} \quad (4)$$

The general theta and delta exponents a and b respectively are given in Table 5, along with the formula for every corrected value. Several pre-conditions are given for the Mach number similarities to be strictly valid, making an impact on the flow field. Mechanical deformation due to stress and thermal expansion on engine hardware are found to have an impact on

aerodynamics. Boundary layer disruption due to Reynolds number effect, and change in the gas constant R due to humidity effects, to name a few. Correction procedures for these effects on the exponents theta and delta are given in [7], but will not be considered further for the sake of simplicity.

Parameter	a	b	Corrected Symbol
Pressure	0	1	$P_c = \frac{P}{\delta}$
Temperature	1	0	$T_c = \frac{T}{\Theta}$
Rotor Speed	0.5	0	$N_c = \frac{N}{\sqrt{\Theta}}$
Gas Mass Flow	-0.5	1	$W_c = \frac{W * \sqrt{\Theta}}{\delta}$
Fuel Flow	0.5	1	$W_{f,c} = \frac{W_f}{\sqrt{\Theta} * \delta}$
Thrust	0	1	$F_{N,c} = \frac{F_N}{\delta}$
Shaft Power	0.5	1	$PW_c = \frac{PW}{\sqrt{\Theta} * \delta}$

Table 5: Parameter correction exponents and formulas [1].

2.4.4 Instabilities

Gas turbines, being a compression system, can exhibit instabilities of different sorts. The two most relevant phenomena are the aerodynamic flow instabilities called surge and rotating stall.

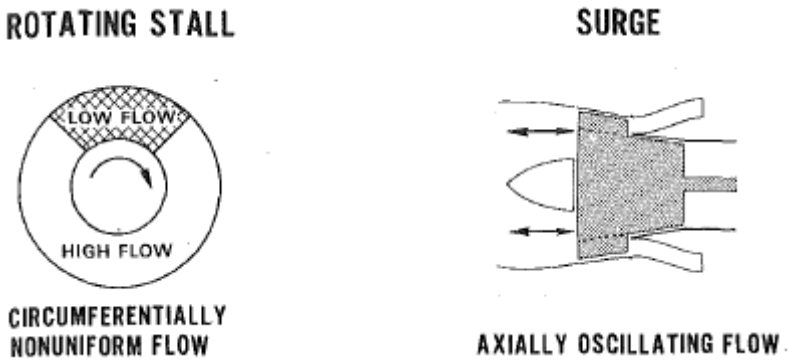

Figure 7: Modes of instability in an axial compressor [8].

Compressor surge is a phenomenon occurring when there is a sudden drop in flow and subsequently delivery pressure to the compressor, and the downstream pressure does not follow

the drop. This forces the air to reverse its direction, see Figure 7, and the pressure ratio drops rapidly making the flow pulsate back and forth in axisymmetrical oscillations.

Rotational stall is induced by the altering in angle of incidence hitting the channels between vanes or blades. Alteration is a result of a breakdown in, or low volume flow for one channel situated between the affected channels, see Figure 7. This is a consequence of non-uniformity in the flow or geometry of the channels, and is often worsened as the stall spreads to neighbouring channels.

Both surge and rotational stall result in instability and poor performance and should be closely monitored and avoided. In the compressor map, surge can be indicated by the lines which the operational point crosses. Vibrations caused by these phenomena can also have non-recoverable results including fatigue failures throughout the gas turbine [3]. They are also reported to heat the blades and increase the exit temperature of the compressor [9]. Anti-ice system alteration of operational point is not sufficient for these instabilities to occur and therefore they will not be included further in this thesis.

2.4.5 Emission control

The gas turbine emissions were not a concern for many years until the understanding of industrial pollution and number of gas turbines increased. Political pressure to minimize the environmental impact through sanctions and taxation, caused the invention of new technologies. First, combustion chamber design was solely responsible for controlling emissions, and the Dry Low Emission combustor [10] was developed. Now control systems capable of adjusting the fuel/air-flow for different operating points are popular. Better understanding of gas turbine degradation [11] due to fouling has also given ground for compressor washing regimes to recover lost performance and reduce emissions [2].

Below a table for emissions to air for three major fossil fuels are given. The relatively low emissions from natural gas combustion compared to other fossil fuels is evident. Nevertheless the numbers, although released in 1998, indicate high costs of maintaining gas turbines offshore with prices of CO_2 and NO_x emissions at 500 $NOK/tonne$ and 21,94 NOK/kg respectively [12].

Pollutant	Natural Gas	Oil	Coal
Carbon Dioxide	50 214,59	70 386,27	89 270,38
Carbon Monoxide	17,17	14,16	89,27
Nitrogen Oxides	39,48	192,27	196,16
Sulfur Dioxides	0,43	481,55	1 112,02
Particulates	3,00	36,05	1 177,68
Mercury	0,00	0,003	0,007

Table 6: Pollutant emissions for fossil fuels in kg/GJ [13].

3. Ice formation

It is important to understand how ice can form on gas turbines and equipment before the specific technologies are considered. This chapter covers how ice forms on different surfaces in the gas turbine and its components, what ambient and inlet conditions contribute to the ice formation and what impact it has on the operation of the whole engine. There are generally two types of icing phenomena.

3.1 Precipitate icing

Precipitate icing includes all forms of free water that can be drawn into the intake of the gas turbine during operation in cold atmospheres. Conditions such as rain, snow, fog ice and hoar frost belong to this mechanism. Though not regarded as critical hazards, as these foreign objects rarely reach the engine itself, they are reasons for concern. Snow and frost can over time accumulate on an exposed surfaces and water can freeze to ice, and then build layers. Rain droplets and fog can load the inlet filter making it saturated and thus increase the pressure drop explained later in the chapter.

3.2 Condensate icing

The phenomenon of condensation in the gas turbine intake happens when air entering the system is pressurized or cooled below the saturation limit or dew point. Below the dew point water molecules will start to cluster making water droplet. The water droplets formed will supercool and turn into ice crystals or stick to a cold surface making condensate. Condensate can as precipitate ice build up in layers as well. The probability of condensation and icing depends on the air humidity and temperature which dictates the saturation limit of the air, see Figure 8. It is important to note that condensate icing does not exist as atmospheric conditions, but is rather induced by the engine system at the atmospheric conditions.

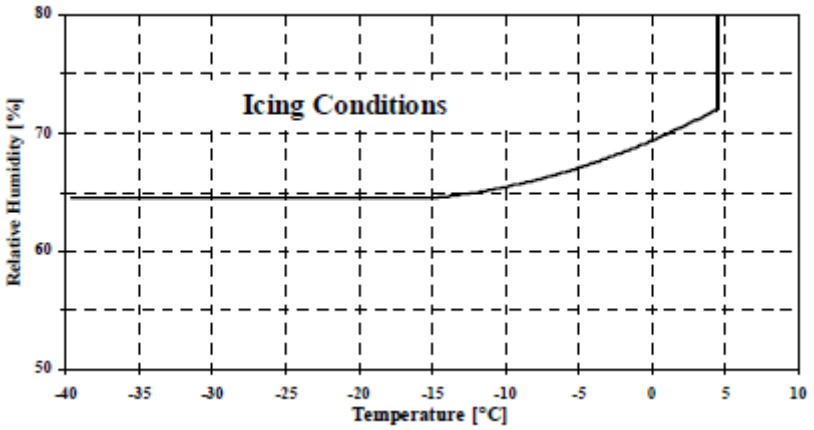

Figure 8: Icing conditions as a function of relative humidity and temperature in ambient air [14].

3.3 Operational impact

Understanding the impacts of the intake system on the inlet conditions is important for understanding the consequences these conditions then have on the operation of the engine. A rapid loss of temperature is often the reason of icing in sections with decreasing cross-sectional area such as gas turbine inlets and especially the bell-mouth. The cross section of the flow is inversely proportional with the flow velocity as given by relation:

$$(AV)_1 = (AV)_2 \tag{5}$$

The Bernoulli's equation gives us the pressure decrease with velocity increase:

$$\frac{v_1}{2} + \frac{p_1}{\rho} = \frac{v_2}{2} + \frac{p_2}{\rho} \tag{6}$$

Pressure loss results in a temperature decrease related by the real gas equation of state:

$$PV = nZRT \tag{7}$$

Z being the compressibility factor compensating for the real gas properties.

The gradual build-up of ice on the gas turbine intake components are often the result of rapid cooling of surfaces due to the above-mentioned effect. With a temperature and pressure drop the saturation limit of the humid air often found offshore will be reached, as described earlier. Combined the water vapour will condensate on these colder surfaces. Precipitation such as sleet snow, freezing rain and fog are also known to cause problems on cold surfaces like this. Combined, these effects escalate the probability of icing. Precipitate icing is particularly apt to

accumulate on components in the compressor inlet such as bell-mouth. Which makes it difficult to foresee as it does not form on upstream components.

Icing of components can severely alter the aerodynamic properties of inlet components, especially the bell-mouth or VIGVs, reducing the inlet flow area. If ice builds up on the fine-tuned compressor blading, there will be an altering in blade profile causing diversification in the flow path. The unbalance like this creates can result in unwanted vibrations throughout the compressor.

Direct ingestion of ice particles can cause foreign object damage as depicted in Figure 9. Gas turbines operate at relatively high rotational speeds and the long thin blades of the compressor can get damaged by ingested ice escaping the inlet filters and screens. Sometimes build-up of ice on compressor inlet components can break off and severely damage the compressor blading (usually identified by a change in operation sound tone). This results in major shutdowns for repair reported by Maas and McCown [15].

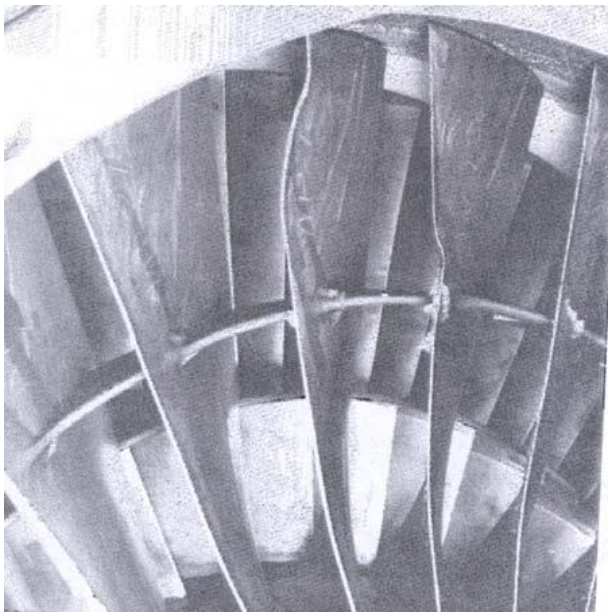

Figure 9: Foreign object damage to compressor blading caused by ice ingestion.

Ice and supercooled water droplets deposited in the air filtration is a common problem illustrated in Figure 10, where cartridge filters mentioned in Chapter 4.1.1 is plugged by frost build up. Consequences of such plugging are poorer air filtration and increase in the pressure drop effect over the filters described in Chapter 4.3.

Figure 10: Picture of ice build-up in cartridge filters [16].

4. Gas turbine inlet systems

This chapter presents an overview of methods for keeping the gas turbine ice free. There are two different terms of icing protection systems. In addition, there are several techniques that inactively hinder ice to enter the gas turbine. Although the last-mentioned techniques do not directly qualify as anti-ice, they play an important role and affect the gas turbine operation. The chapter ends in a discussion of operational impacts of the discussed systems.

4.1 De-ice systems

De-ice systems include all protection systems that promote removal of ice before it can reach hazardous proportions, although some ice accretion is permitted. This entails all mechanical solutions e.g. mechanical and electrical brushing of hoarfrost. Even though de-icing systems are not relevant for this thesis on their own, a small selection will still be included as they are relevant to ice formation and the completion of full ice preventing systems.

4.1.1 Particle filtration

Particle filtration systems are mainly made to filter out contaminants from the intake air, but as they are made up of finely knitted filter elements they catch water droplets and ice particles. A filtration configuration can vary between locations and manufacturers, but it usually consists of pre-filters, high-efficiency filters, and a vane separator.

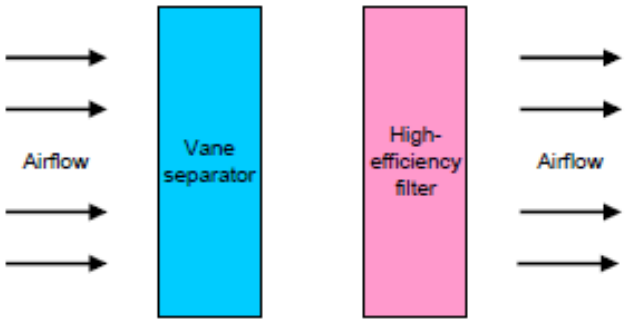

Figure 11: Filtration configuration deployed offshore.

As mentioned in Chapter 3, the obstruction of air and subsequent pressure and temperature loss is increasing as the efficiency of the filtration is increasing [16]. This seems to be strengthened by the addition of water and ice saturation in the filter. Therefore, all air filtration systems in industrial gas turbines are careful trade-offs depending on location and ambient conditions.

The systems are made up of several stages of particle filters in the intake of the gas turbine. The first filters' duty is to catch larger particles, the efficiency of the next filters increase

downstream as the particles decrease in size. As the filters get more saturated the pressure drop will increase and a pressure sensor downstream will trigger a cleaning procedure. The procedure is either done manually or automatically by pulses of air blown in reverse direction by jets. Filters such as the cartridge filters shown below (Figure 12) are cleaned by this last-mentioned method.

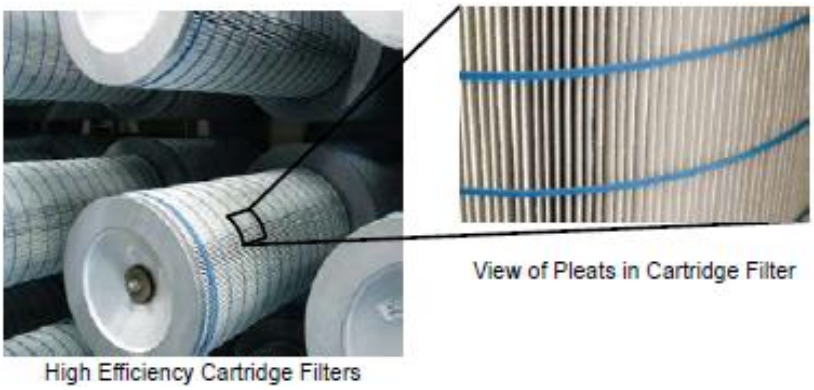

Figure 12: High efficiency Cartridge Filters

Ice and vapour build-up in the filters is a common problem and the heating of the inlet air will help to keep it under control. The warmer air melts the ice and further dries out the liquid stuck there, decreasing the pressure drop effect.

4.1.2 Other inlet air treating systems

An active protective system is crucial for preventing ice in the machine, but there are measures that can be made to enhance the operation. In the first stage of inlet, defence hoods which deflect the intake air upwards, forcing heavy rain droplets to settle and drain away are installed for a gas turbine (depicted in Figure 13). Second, instalment to the first stage defence can be bird screens or moisture separators, these induce several directional changes to the inlet air that the heavier moisture and small liquid droplets are unable to follow due to gravity. Depending on ambient conditions, several stages of moisture separators can be installed.

Figure 13: Inlet hoods on offshore gas turbine.

4.2 Anti-ice systems

Anti-ice systems are used for all protection systems preventing the ice to form on the gas turbine intake surfaces or preventing precipitate icing to reach the compressor. A relevant selection of systems will be covered on the following pages.

4.2.1 Compressor inlet bleed heating systems

The most frequently used anti-ice system installed today is heated compressed air bled of a intermediate compressor stage or at discharge. Compressor bleed air is generally used for multiple purposes. Extracted from earlier stages, the relatively cold compressed air serves as cooling medium for the turbine blades, but the air can also be utilized as driving medium for other equipment or as surge control, see Chapter 2.4.4. In the LM2500 using this technique, the air is vented of the 16^{th} stage in the compressor. This, approximately 700 K, air is mixed upstream the inlet filters in the gas turbine intake, although there are some systems that inject after the inlet filtration. The system requires only one control valve to function and increases the inlet air above the condensation and icing limit, usually 5-10 K. High pressure ensures satisfactory mixing in the intake, leading to no local cold regions to form. Inexpensive and simplistic, this method has also proved to have great reliability in the cold climates of the northern hemisphere [17].

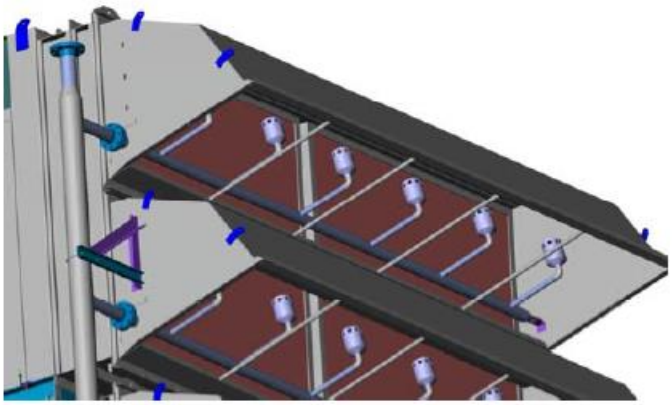

Figure 14: Injection of hot bleed air at the inlet hoods in the gas turbine intake.

Part of the success of this system is because the compressed warm air, being dried, adds no moisture to the inlet air of the gas turbine. Dryer air keeps the relative humidity below condensation condition, see Figure 8. Moisture slipping through the first stage inlet prevention system saturating the inlet filters, will be removed by this dry warm air. Figure 15 shows the schematic of a typical bleed air system supported by a self-cleaning filter compartment. Inlet filtration is covered in Chapter 4.1.1.

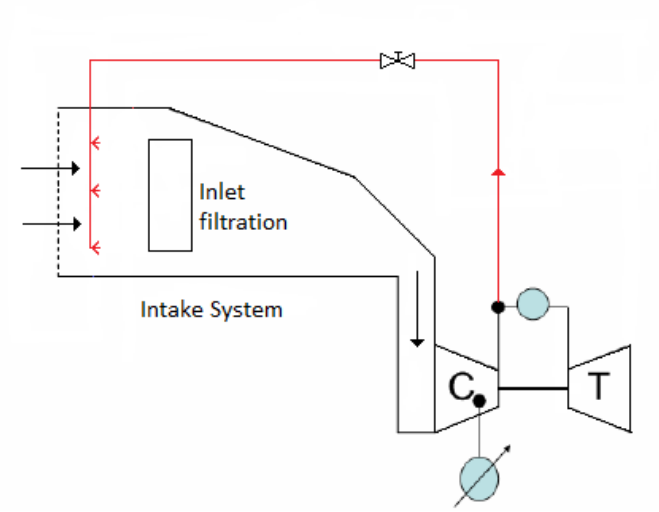

Figure 15: Simplified schematic of a hot bleed anti-icing system.

4.2.2 Waste heat recovery system with heat exchanger or radiator

An anti-ice method utilizing the hot exhaust gas, approx. 1100 K, from the power turbine is shown in Figure 16. The technology bypasses the problem of bleeding of crucial air from the compressor and instead uses other mediums for heat transfer via heat exchanger or radiator. This prevents direct injection of exhaust gas which contains combustion products fouling the compressor. Several configurations use this method. Figure 16 displays heated compressor air vented before the inlet, resulting in no reported losses to the performance, and redistributed further upstream near the intake. The exhaust gas is then sent to the atmosphere [18]. There is not enough pressure to drive the air through the heat exchanger and therefore a fan is installed, promoting additional power and place demand.

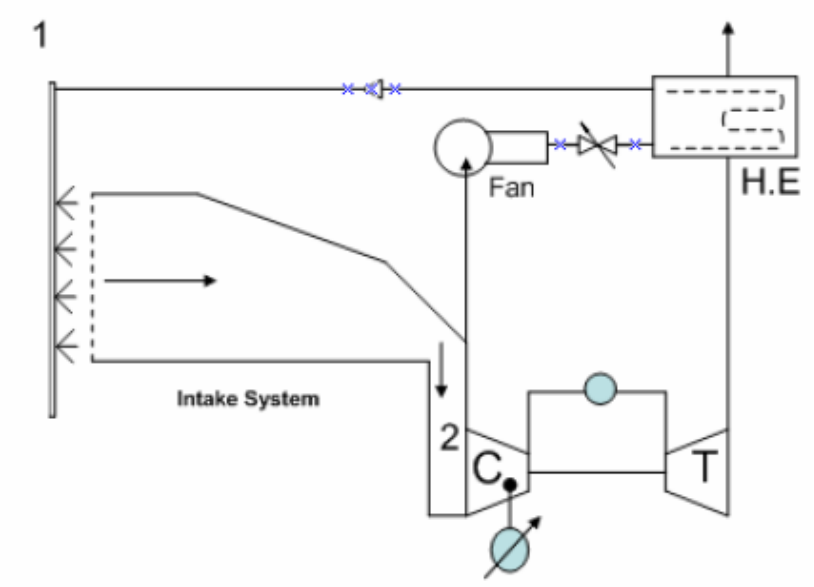

Figure 16: Simplified schematic of waste heat recovery anti-icing system utilizing inlet air as medium.

Another newer configuration which is utilized offshore is placing the radiator in the intake and circulating a transfer medium heated by the exhaust gas. This makes good use of the exhaust gas while simultaneously not venting off any compressor air. After the heat has been transferred by convection, the exhaust gas is sent to the atmosphere, see Figure 17.

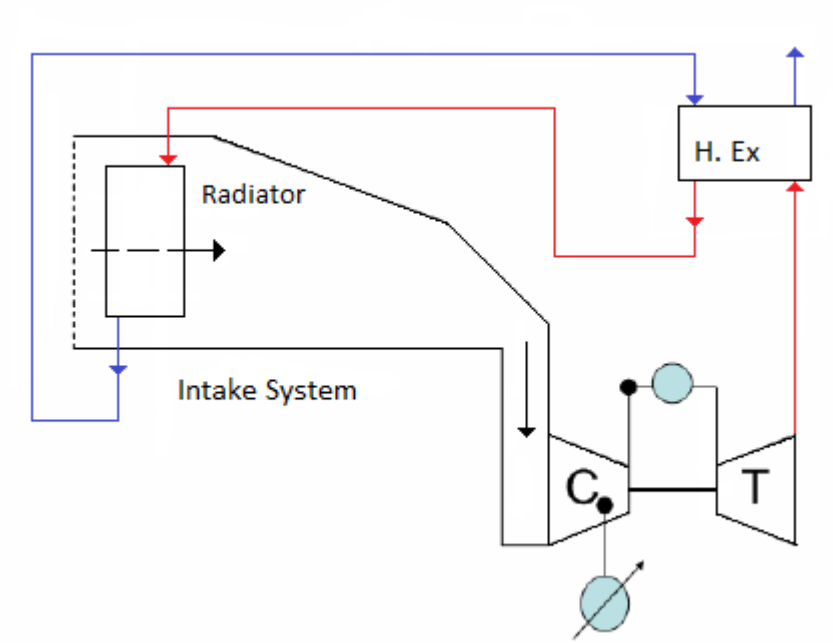

Figure 17: Simplified schematic of waste heat recovery anti-icing system utilizing transfer medium.

Both configurations of the exhaust recovery system have lower impact on the performance as they do not bleed of compressor air, but the intake air is still warmed up, decreasing the overall thermal efficiency. This is documented thoroughly by Hadik [19]. There are also some other disadvantages in complexity and cost, and the sheer volume of the system, which are important factors especially on offshore platforms where space is limited [20]. A closer look at the operational impact of the last-mentioned system will be given later in this chapter.

4.2.3 Exhaust recirculation system

One of the easiest and most affordable methods of preventing ice today is to recirculate the exhaust gas directly into the intake, mixing it with cold intake air. An immediate problem with utilizing exhaust gas is the impurities of combustion products still left in the gas and the danger of further compressor fouling [18], which is why it is mostly replaced today by the systems previously mentioned. Even though gas fired gas turbines produce less particles, the exhaust gas still contains approx. 3 % water vapour [21] which increases the relative humidity and promotes icing.

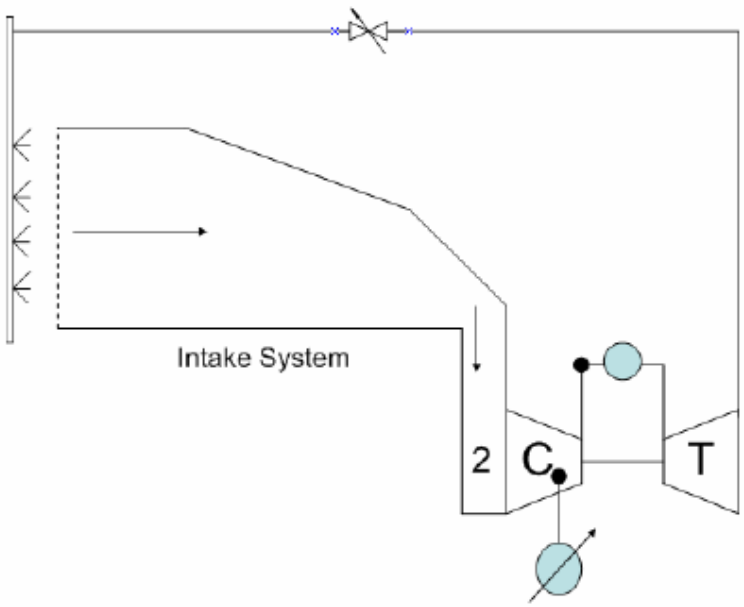

Figure 18: Simplified schematic of an exhaust recirculation anti-icing system for a gas turbine.

4.3 Operational Impact

A simplified schematic of the hot bleed system is depicted in Figure 19. When the bleed valve is opened, two important effects contributing to altered thermodynamics,z take place. The effect reserved specifically for hot bleed air extraction is the decrease of mass flow to the combustion chamber and the following GG turbine, but also the increase in mass flow for the compressor. As the matching of flow and power balance between the GG and PT is altered, the equilibrium line with operating points for the compressor shifts, as depicted in Figure 20.

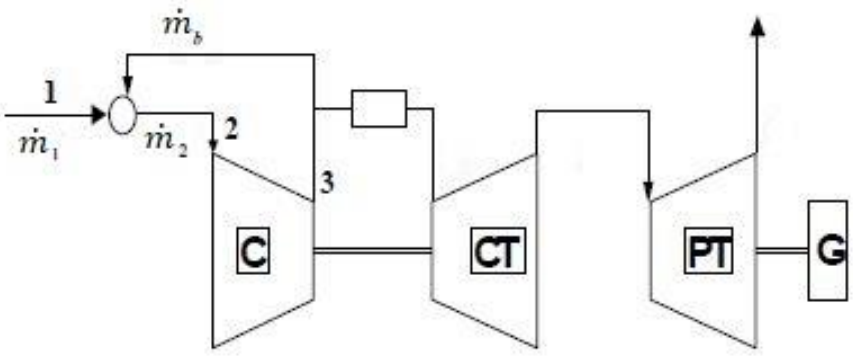

Figure 19: Simplified schematic display of hot bleed anti-ice depicting the mass flows.

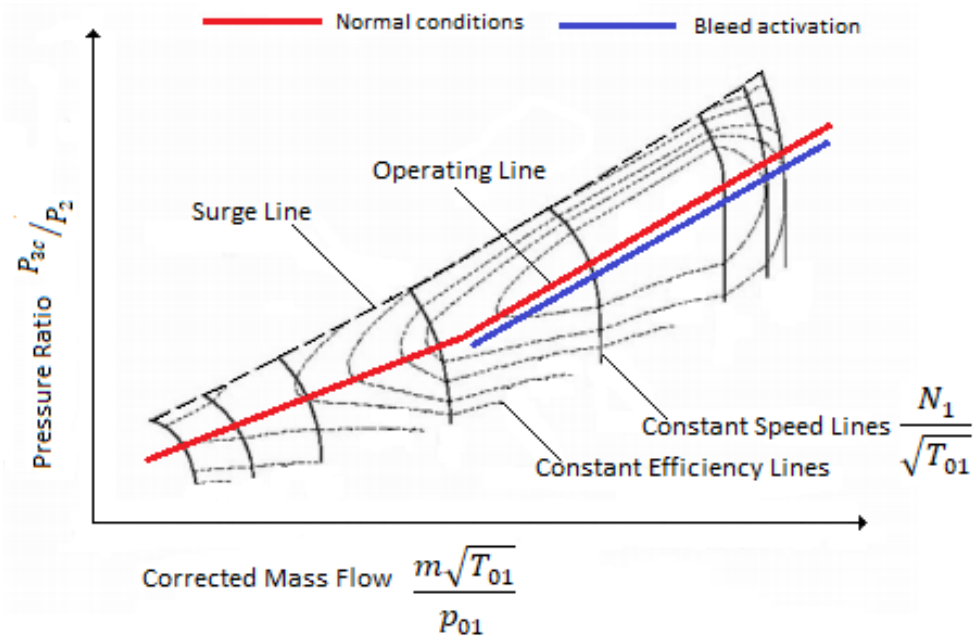

Figure 20: Compressor map displaying alternative equilibrium line due to anti-ice activation.

As can be seen from the compressor map (Figure 20) the activation of bleed is resulting in a general decrease of pressure ratio, but where on the blue equilibrium line the operating point will end up is dependent on the mode of operation (constant load, speed, exhaust gas temperature etc.) This can also be explained by the thermodynamic relation (Equation 2) between temperature and pressure, leading to the second effect of inlet temperature rise in the compressor. It has been documented [22] that effects on the operational parameters such as GG speed, discharge temperature and thermal efficiency is evident, and that thermal efficiency decreases as inlet temperature increase [19], while keeping TIT constant, see Equation 3.

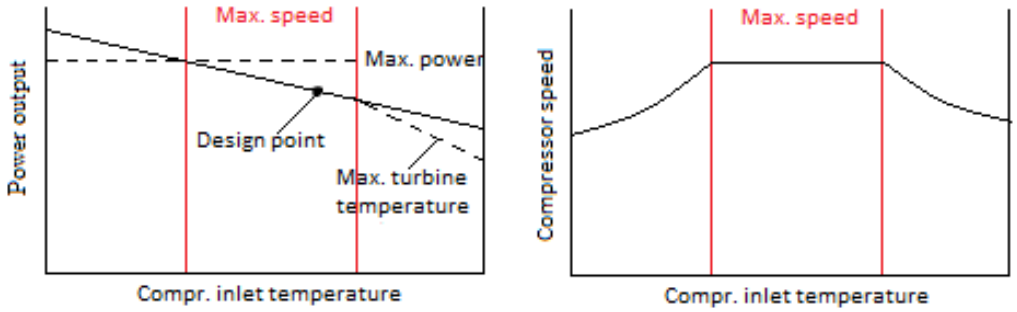

Figure 21: Plots showing control system response to higher inlet temperature [2].

When compressor inlet temperature increase following anti-icing activation, the control system increases the speed, and when maximum speed is reached the power is decreasing. Figure 21 explains this. The left graph shows the power limitation of increasing the compressor inlet temperature, and not damaging the turbine with too high exhaust temperatures. Right graph

shows the GG speed limitation, indicating a reduction in speed after a certain inlet temperature is reached. Some suggest a loss of performance ranging from 2 to 5 % [20]. Therefore, several studies have proven that significant amount of power can be saved by optimizing limits in which especially bleed air system operates [23, 24]. It is important to note that the temperature increase experienced by the compressor explained above is applicable to both hot bleed- and waste heat anti-ice systems.

The inlet filtration system constricts the flow creating a static pressure drop in the compressor inlet flow, decreasing the delivered pressure and hence the density of the inlet air to the compressor, see Figure 22. Monitoring the drop can be utilized for condition control of the filter.

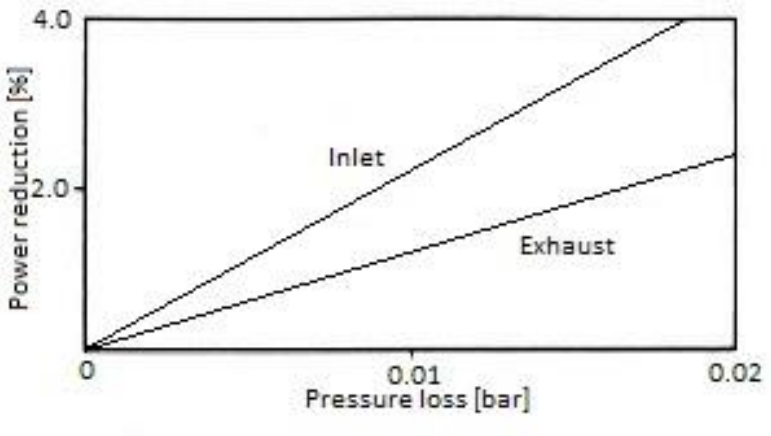

Figure 22: Power loss induced by pressure loss at inlet and exhaust, derived from Øverli [25].

This effect results from filter efficiency as the filter resistance factor is higher. Because the filter condition is monitored closely, it is commonly assumed that the intake system will experience a slow and steady increase in pressure drop as the air filters become saturated with particles and sometimes ice, described in Chapter 4.1.1.

4.4 Summary and conclusion

This chapter has focused on different anti-icing technologies and their functionality. Emphasis has been put on deciphering their operational impact, through literature review, as these parameters often advocate what technology must be utilized. Some weight has been put on air filtration and additional inlet systems as they are vital to optimal icing prevention system performance.

From this review it can be recommended to install an anti-ice and a filtration system working in tandem installed. Keeping the icing formation theory in mind, the intake system should be

able to handle both precipitate- and condensation icing. For precipitate icing the filtration configuration may vary depending on location but decisions should be based on filtering out most ice, snow and fog ice reaching the compressor bellmouth. This will reduce the need for inlet heating which only activates when icing conditions are met. Balanced with the pressure drop connected to high efficiency filters, a self-cleaning mechanism is recommended e.g. cartridge filters.

As the filtration system will be loaded with ice and possibly slush, the inlet heating anti-icing system should be installed at the intake, see Figure 10 and 14. This ensures that the pressure drop is controlled and increase filter lifespan. The main reason for heating the inlet air is to prevent condensation of water vapour and icing from supercooled water. Waste heat recovery systems utilizing a radiator at the inlet is further recommended due to obvious performance advantages vs. the hot bleed system, although the instalment is costlier. Some performance deterioration stemming from inlet heating should be expected and the activation limits should be optimized.

Other preventive systems of simpler design such as inlet hoods and moisture coalescer are recommended. These measures will prevent most of the rain and snow to enter the intake if the quantities are high, and keep moisture and small liquid droplets from causing serious corrosion or ice formation downstream. It will also lighten the load of the filters.

5. Analysis of different systems on performance and emissions

Although the anti-icing systems are preventing icing in the gas turbines they will lead to higher inlet temperatures and altered delivered mass flow, impacting the performance of the machines. These impacts and their consequences are important to document and analyse in order to better understand their operation. This chapter focuses on the most used bleed air system and the new exhaust recovery system utilizing a heating medium.

5.1 Presenting results

Analysis of operational data is done in excel, a powerful tool for handling huge numbers of data. Datasheets containing operational data from two gas turbines with two different ice prevention systems and loads are chosen as basis for this analysis. It is important to ascertain how the engines respond to the activation, but also what happens when their ability to adapt to the change is altered. How a gas turbine adapts to different operating conditions depend on the control system, as explained in Chapter 2.3.5, and the engine load.

The ice prevention systems and the subsequent findings are represented hereafter in tables measuring relative change, see Equation 8. Different engines have varying absolute values and are therefore of no comparable interest. The reference baseline conditions are defined as steady state pre-activation mean values. There are both monitored and corrected values in the tables to display the difference and to emphasize the difficulty of accurately analysing and diagnosing these systems.

$$\Delta Y = \frac{Y_0 - Y_{ref}}{Y_{ref}} \tag{8}$$

The changes are thereafter presented in general compressor and turbine maps to display the relative impact on the rest of the gas turbine. It is important to ascertain where the operational point will move and how the equilibrium line will shift, to understand the successive impacts on the HPT and PT in the engine. It is important to emphasize that gas turbine maps are unique to every engine and therefore the maps presented will deviate in detail, but in this thesis the maps are only used to display basic principles and therefore assumed applicable.

5.2 Effect of hot bleed anti-ice system

As explained, when the ambient temperature and pressure drops sufficiently, see appendix D, the probability of icing in the gas turbine increases, and the hot bleed anti-ice system is activated. The effects of the warmer compressor inlet temperature and the air extraction is displayed below in Figure 23.

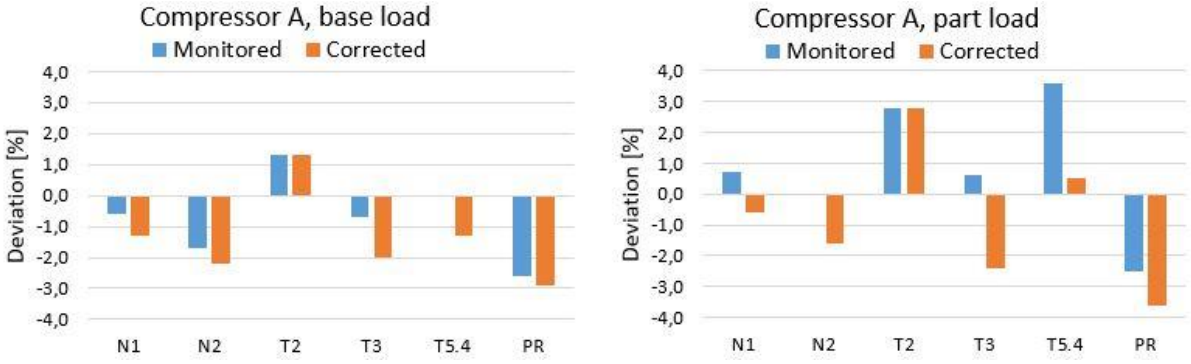

Figure 23: Relative change in monitored/corrected values of compressor A after Anti-ice activation.

Keeping in mind Chapter 2.3.5 and the control systems ability to compensate for warmer T_2, the differences in load are displayed as expected. The performance parameters N_{1c} and $T_{5.4c}$ have both reached and surpassed their upper limit and will either stop or drop for base load. The part load running engine will compensate the T_2 rise and subsequent drop in mass flow by raising them instead. N_{2c} reduction, resulting from less air delivered to the combustion chamber and turbines, will decrease the overall power output and efficiency of the engine. T_{3c} is also experiencing a dramatic drop for both loads.

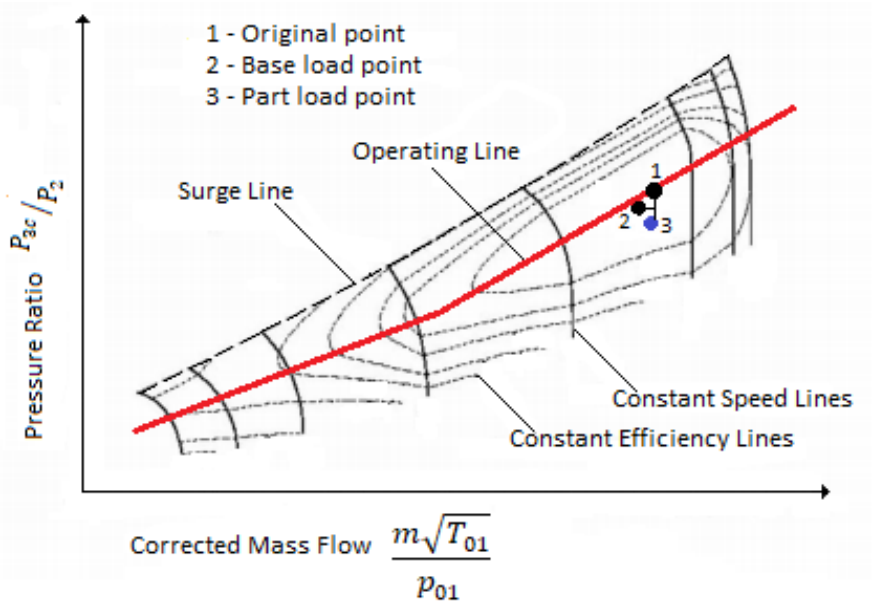

Figure 24: Compressor A map displaying operational point movement due to anti-icing.

Looking at the compressor map given in Figure 24, the operational points change as described in Figure 20. After the engine has gained a steady flow, the point will stabilize on a new equilibrium line where the GG and PT are trying to establish a match. These lines will run through the new points parallel with the original one (red) as described in Figure 20. The drop in pressure ratio and speed moves the operating line away from the BEP, and according to Mckee [26] this indicates a drop in corrected mass flow, and subsequent power output.

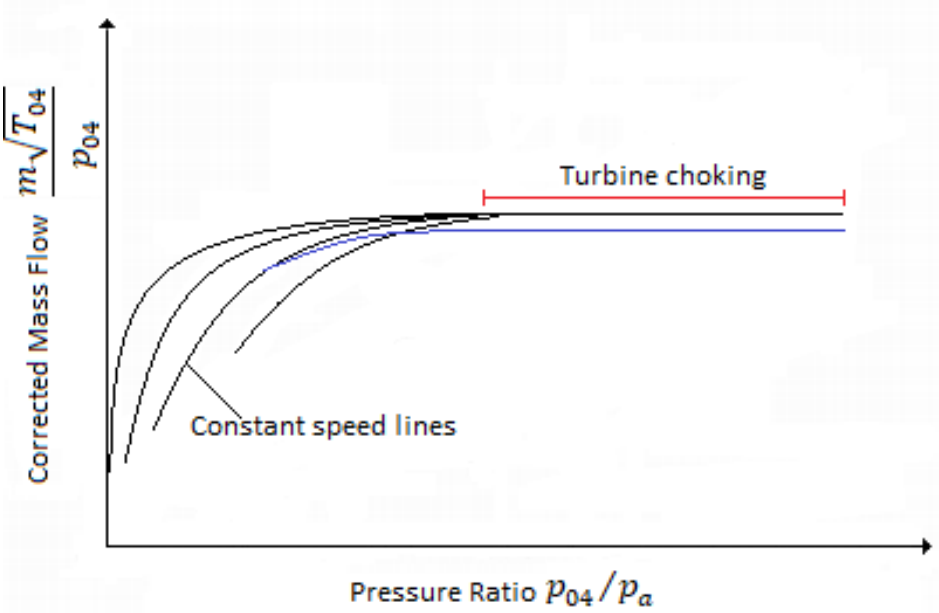

Figure 25: Turbine map displaying the new blue operating line for power turbine A.

In the turbine map the impact of the mass flow extraction becomes evident as the mentioned delivered flow to the turbines decreases. Lower flow to the HPT, depicted by the blue line in Figure 25, will decrease the speed of the whole GG depicted in Figure 24. Incompatibility between the speed and flow in the GG is interrupting the balance between the compressor and HPT. When less flow is delivered to the PT the speed N_2 and subsequent power output drops.

It is important to note that base load bleed valve is opened 10 % only, as opposed to part load 20 %. This results in T_2 differences of 1.3 % and 2.8 % respectively, which might explain some differences in results.

5.3 Effect of waste heat recovery anti-ice system

As explained in Chapter 3.3, when the ambient temperature and pressure drops sufficiently, the probability of icing in the gas turbine increases, and the waste heat anti-ice system is activated. The waste heat anti-ice system is utilizing a radiator in front of the air filtration and the effects are displayed below in Figure 26.

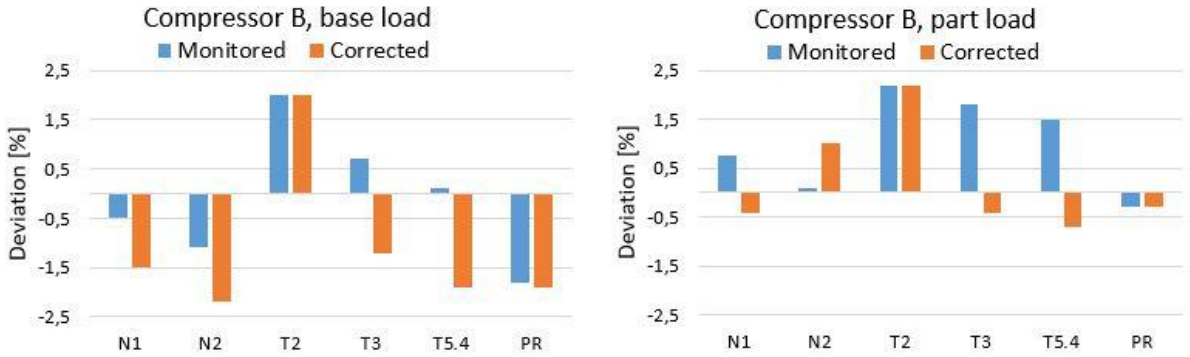

Figure 26: Relative change in monitored/corrected values of compressor B after Anti-ice activation.

Similar trends for compressor B as for compressor A. Base load engine is prohibited from increasing N_{1c} and $T_{5.4c}$, the T_3 decreases as well indicating, together with lower PR, lower compressor work.

Part load does not experience this restriction and the trivial T_3 and PR decrease indicates pressure and temperature maintained due to small N_{1c} dip and a rise in N_{2c} which is exclusive to this engine and load. No clear trend for $T_{3c}$is possible to ascertain for both loads, but some slight change in base load is visible.

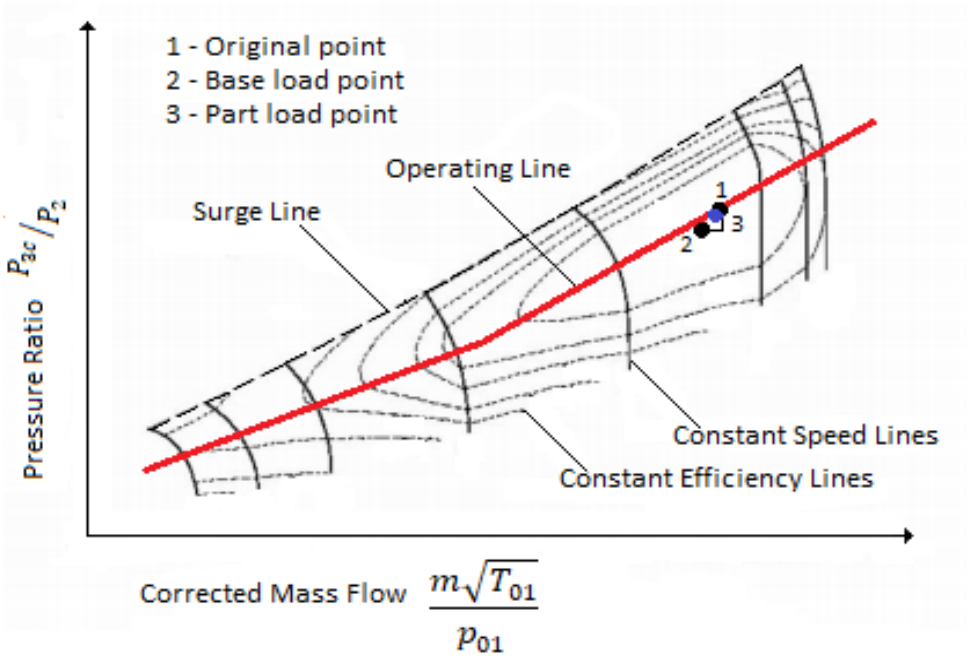

Figure 27: Compressor B map displaying operational point movement due to anti-icing.

It is important to note that for a relatively similar T_2 increase, compressor B suffers a generally modest change in PR, an important performance parameter. $T_{5.4c}$ is also lowered, which indicates a decrease in fuel flow.

The operating points of the compressor map suggests a similar movement away from the original operating line as the hot bleed, but of more modest magnitude. The new lines will be established parallel to the original one (red) and the corrected mass flow will be reduced as an effect of these drops of PR and N_1. Looking at the efficiency lines the operating points will move outward towards lower efficiency and away from BEP.

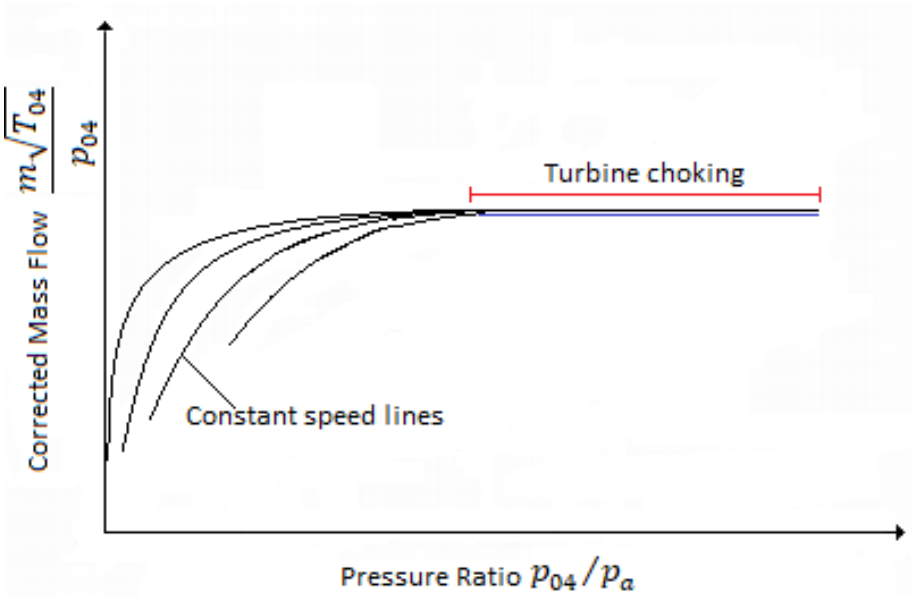

Figure 28: Turbine map displaying the new blue operating line for power turbine B.

From the turbine map it is possible to detect a small change in the mass flow to the PT as the N_2 parameter is reduced in the base load run. This stems from the increase in inlet temperature, which decreases the density and therefore the speed of both GG and PT indicated by the blue line in Figure 28.

5.4 Emissions

As described in Chapter 2.4.5 the emissions to air are highly connected to certain operation parameters. Bakken [11] reported that discharge pressure and fuel/air-ratio and subsequently the combustion temperature of the gas turbine, specifically affect the formation of airborn particles.

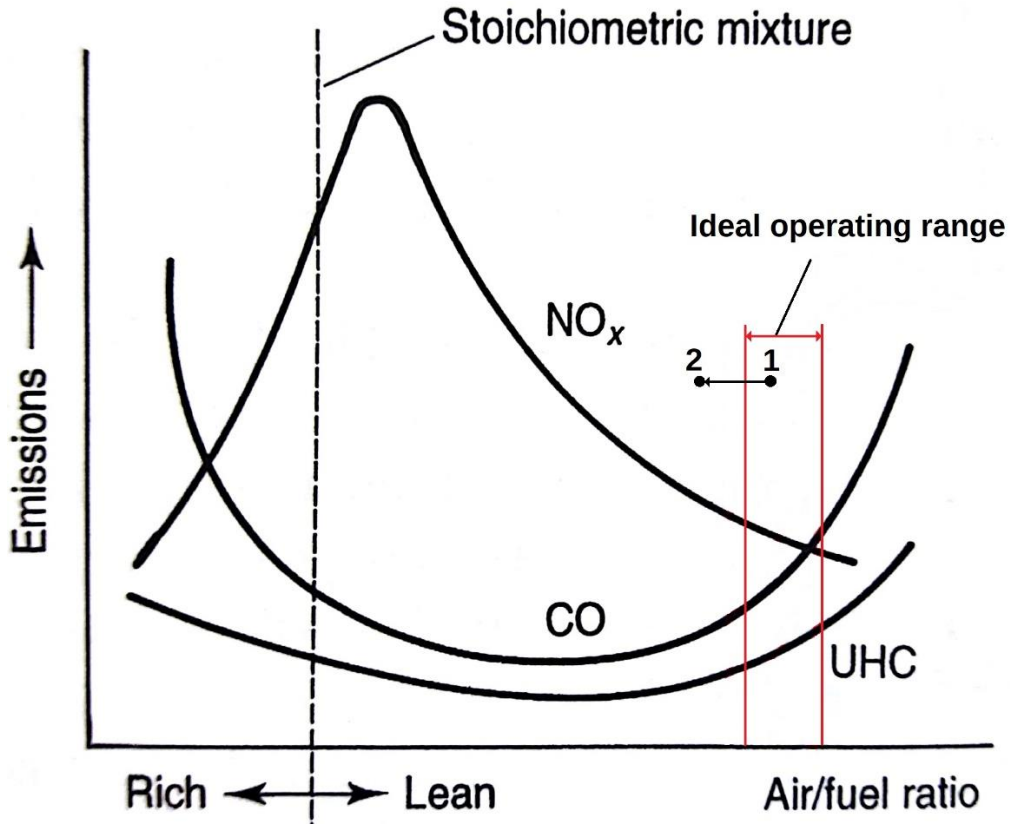

Figure 29: Gas Turbine Emissions of CO/NOx/UHC as a function of combustion temperature and fuel/air-ratio.

Figure 29 depicts the emission balance between CO, NOx and UHC particles as a function of fuel/air ratio and combustion temperature. As mentioned earlier the air extraction and warming of T_2will decrease the combustion chamber mass flow resulting in higher fuel/air ratio. This shift will move the operating point in the emission chart past the desired range of combustion temperature (point 1 to 2), resulting in higher emissions of especially NO_x to the air, increasing taxation on operation significantly.

Another important factor influencing the combustion flame, and therefore the emissions, is the discharge pressure P_{3c}, as both the pressure and temperature into the combustion chamber influence the diffusion flame temperature. The Pressure ratio is inclining in 3 out of 4 cases in the analysis and it is concluded it will reduce the NO_x by a small degree according to scaling laws suggested by Røkke et al. [27].

5.5 Instrumentation

The accuracy of the instrumentations are important factors to consider. The two gas turbines are equipped with two different sets of instrumentation that have relatively large differences in accuracy. Gas turbine A has the newest instrumentation and therefore a more precise reading of its measurements.

A sensitivity analysis has been conducted in previous work [2] to see how this difference in accuracy affects the operational data. The analysis is based on datasheets containing information on the pressure instruments of both engines, both new and old. The deviation in input, meaning the ± confidence interval given, is plotted against the resulting deviation in output parameter chosen to be efficiency.

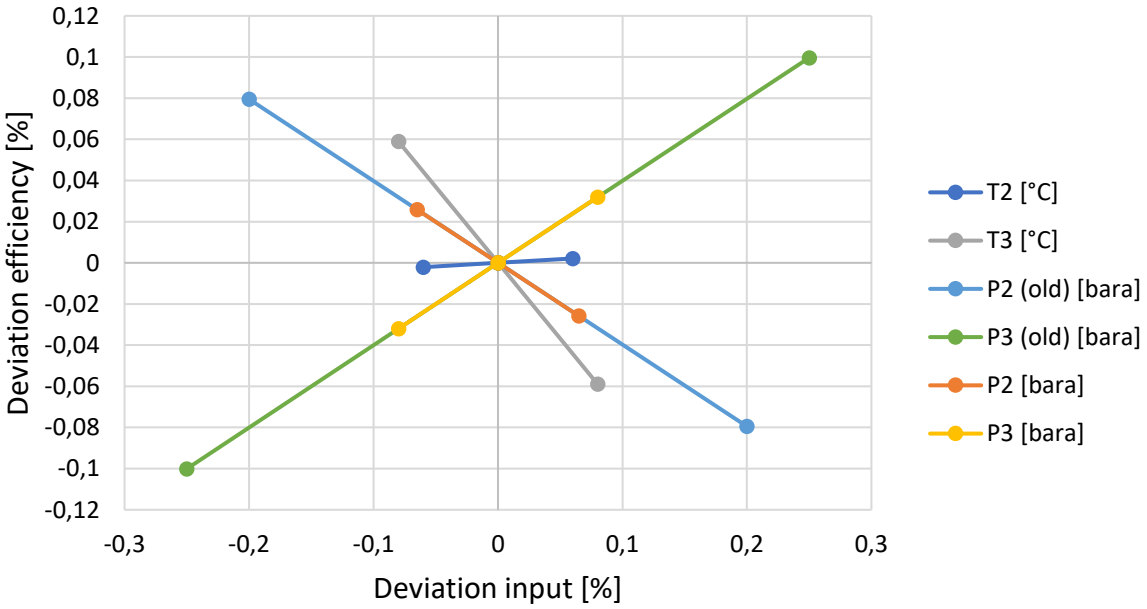

Figure 30: Deviations of efficiency vs. input deviations due to instrument uncertainty[2].

The results are shown in Figure 30, where the old (light blue and green) and new (red and green) pressure instruments for the two gas turbines are clearly visible. The different results indicates how important it is to have state-of-the-art instrumentation to get reliable measurements and how difficult performance readings can be for gas turbine B.

It is also interesting to see how different the four parameters vary in impact on the polytropic efficiency and, in accordance with Samnøys [28] findings, especially T_3. It is important to emphasise that the confidence interval portrayed for the temperature measurements are assumed and not given, and are included for the sake of comparison. The confidence intervals are assumed the same as the pressure instruments.

5.6 Turbowatch validation

To validate the monitored results coming from offshore software Turbowatch, the results are tested through a compressor model in HYSYS. With the use of Aspen Simulation Workbook the values in excel are easy to export to the simulation model, shown in Appendix A.

The simulation program employs the Soave-Redlich-Kwong (SRK) equation of state (EOS) for describing the relation between state variables and physical parameters. Details on the SRK EOS is described in Appendix B and it is the preferred EOS of NTNU for compression simulations.

When calculating for polytropic flow in thermodynamic machinery, it is important to account for real gas relations. In this simulation the real gas calculations of Schultz [29] are chosen for the calculation procedure. It differs from ideal-gas relations by supplementing compressibility factor Z with compressibility functions X and Y. It also introduces a polytropic head factor f to adjust the results for deviations from ideal-gas behaviour. Schults' method proposed a simple iterative way of accounting for real-gas relations in the calculations, see Appendix C.

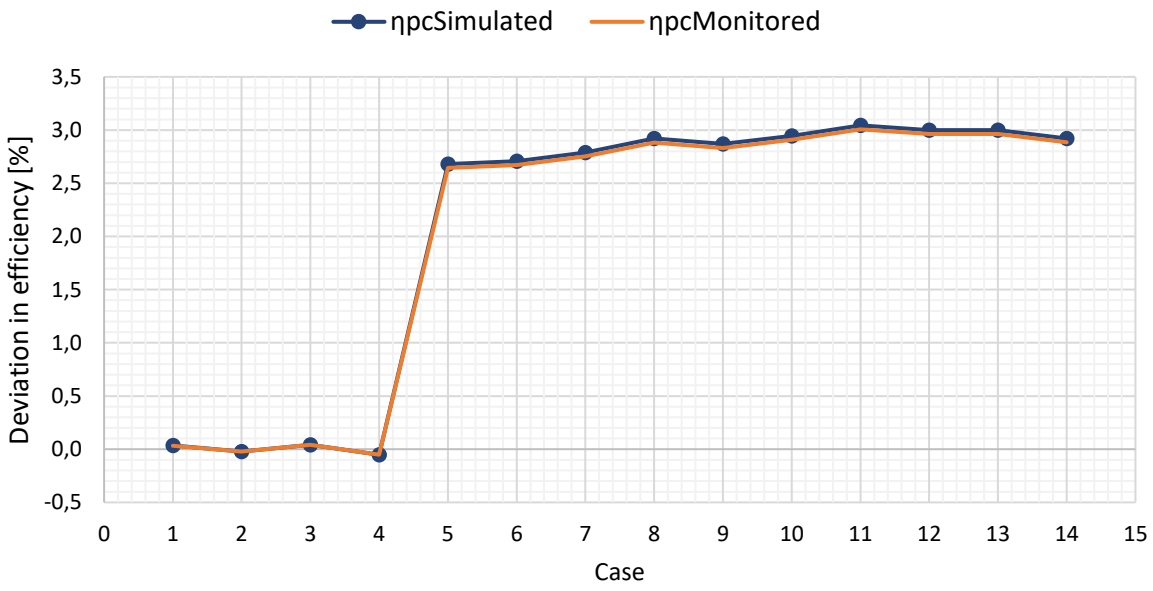

Figure 31: Calculated vs. simulated polytropic efficiency for compressor A.

As can be seen from Figure 31, the efficiency trends are near to identical. The absolute values of the trends deviate by a small degree, which is expected due to differing EOS. Therefore, the relative values of deviation are very similar and consistent. This leads to the conclusion that the data from Turbowatch is representative and applicable for further analysis, if the EOS stays the same and the interest is in relative change.

5.7 Summary and conclusion

In this chapter, two gas turbines with two different anti-ice technologies have been analysed to better understand the impact of their operation. The two gas turbines are of the same LM2500PE type and are therefore assumed comparable, although differing locations, atmospheric conditions, applications, and instrumentations cause some uncertainty in the results. It is important to emphasise that it is difficult to analyse these machines because the results are inconsistent. However, the differences between the load run of the engines and the ice prevention principles show some interesting results.

The hot bleed activation of gas turbine A displayed a vast increase in inlet temperatures and decrease in mass flow, indicated by lower N_{1c}. Mass flow is delivered to the downstream components and the PT rotational speed N_2 and subsequent power output is decreased. This effect is noticed in gas turbine B, indicated by the T_2 rise, although at a smaller rate. Compressor B with no flow extraction confirms these relatively small changes in performance parameters and power output. Pressure ratio is the clearest indication of decrease in performance as indicated in the compressor maps. Compressor A has the highest decrease in delivered pressure ratio of the two engines, which is a result of the mass flow extraction. Compressor B even employs constant PR throughout the activation. The pressure ratio is also impacting the downstream components as performance of the turbines are heavily dependent on the available pressure delivered. This fact is important because the effect of a pressure loss depends on the pressure level at which it occurs, which is high for the LM2500PE.

Higher fuel/air ratios produce a higher NO_x concentration in the exhaust emissions as the operating point moves away from the ideal operating range depicted in Figure 29. On the other hand, a drop in pressure ratio will reduce the NO_xemissions slightly.

Reduced drop in important performance parameters throughout the gas turbine, lower inlet heating of the air and reduction of NO_x emissions are clear advantages of choosing the gas turbine B's waste heat recovery system. The analyses done in this chapter confirm the conclusion in Chapter 4.4 even though important performance parameters such as mass and fuel flow and TIT were not provided. Some uncertainty must be addressed considering the poorly instrumented gas turbine B and upgrading these instruments are recommended.

6. Correction of anti-ice system impact on performance

It has become apparent throughout this project that a procedure of correction for the efficiencies of the gas turbine, when bleed air anti-ice system is activated, is sorely needed. This chapter suggests an additional procedure for correcting the altered efficiencies for air extraction by establishing correction factors. The chapter then suggests the procedure and ideas for further work.

Note that only representative steady state measurements are included in the graphs and calculations in this chapter. Due to heat transfer to cooler ducting, the initial period of bleed valve opening is irrelevant for analysis and correction. For simplicity's sake, 14 representative cases were chosen and run through the simulation model in HYSYS to implement real gas relations according to Schultz and the SRK OES, see Chapter 5.6.

6.1 ISO standard correction for performance

Chapter 2.4.3 cemented the standard correction method based on Mach number similarities as an accepted way of accounting for varying inlet conditions. These inlet conditions being temperature and pressure, were used to produce operational parameters comparable to test results. From there the real performance of the engine can be found.

6.1.1 Polytropic efficiency

Figure 32 displays the corrected compressor performance measured in polytropic efficiency.

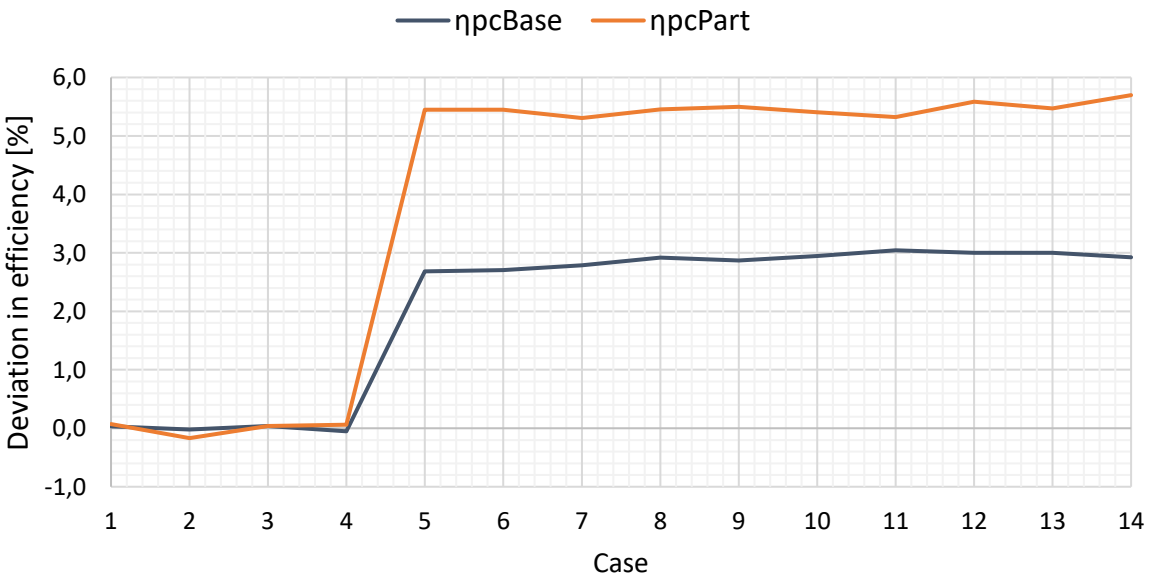

Figure 32: Display of polytropic efficiency deviation in corrected base and part load parameters when hot bleed is activated.

As can be seen in Figure 32, the ISO standard method of correction do not suffice in sorting out the deviation. In theory the polytropic efficiency will be kept constant throughout the activation period, but this does not happen. Other correction measures are required. To illustrate this further the compressor map depicted in Figure 24 has the point of operation shifted even though the inlet changes have been corrected for. This shift is due to altered N_{1c} and PR_c. The second effect mentioned in Chapter 4.3, covering the extraction of compressor mass flow which alters the GG balance, needs to be addressed and subsequently corrected.

6.1.2 Thermal efficiency

Figure 33 displays the corrected gas turbine performance measured in thermal efficiency.

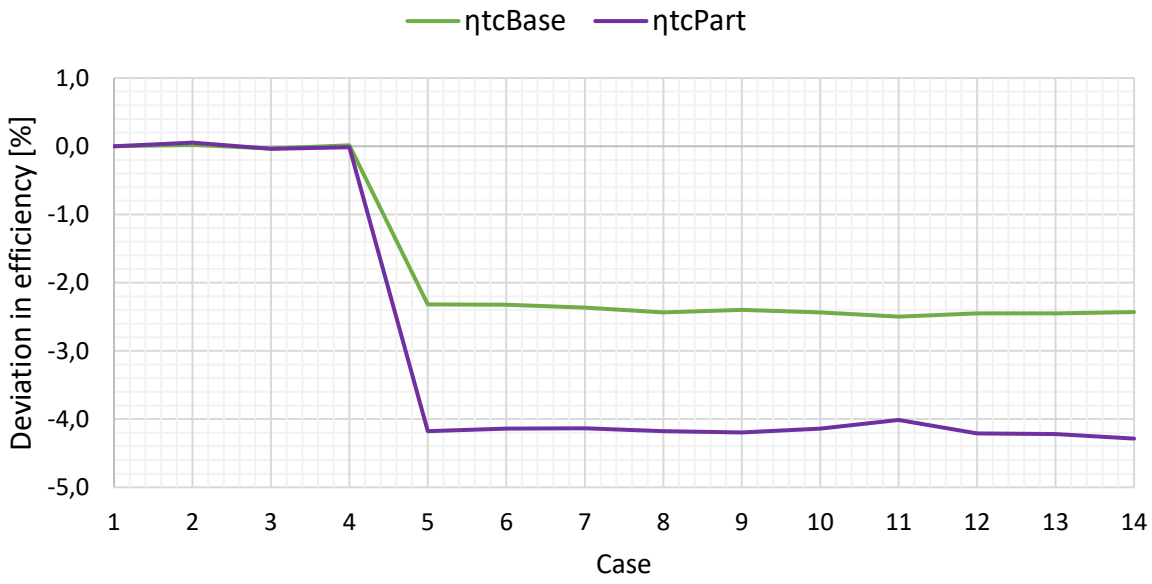

Figure 33: Display of thermal efficiency deviation in corrected base and part load parameters when hot bleed is activated

The thermal efficiency of a gas turbine will under normal circumstances drop slightly when T_2 increases. As can be seen from Figure 33, a drastic drop especially for part load indicates that other circumstances are affecting the results, such as the flow extraction. The flow extraction will reduce both pressure and temperatures discharged from the compressor. Reducing the T_{3c} will require an increase in fuel flow to the combustor, reducing the thermal efficiency as explained in Chapter 2.4.2.

6.2 Correction procedure

Procedures utilizing correction factors are widely used within several engineering disciplines to siphon out external noise, that affects the final measurements and consecutive results. This is done by analysing operational parameters and ascertain what parameters coincide with the deviation in trend. Supported by theory, these parameters make up correction factors, $K_1, K_2, .., K_n$, which together with the efficiency parameter, $Y_{measured}$ in this case, makes a corrected parameter $Y_{corrected}$.

$$Y_{corrected} = Y_{measured} \cdot K_1 \cdot K_2 \dots K_n \quad (9)$$

The correction factors K_n from Equation 9 correcting for the chosen parameters can be calculated from Equation 10. This equation is derived from Salit et al. [30], where ΔY_i can be found by Equation 8.

$$K_i = (1 \pm \Delta Y_i) \quad (10)$$

6.2.1 Polytropic efficiency

Correcting for the air extracted from the last stage of the compressor, the mentioned compressor map, Figure 24, gives important clues. The movement of the operating point away from BEP is credited two corrected operational parameters, PR_c and N_{1c}. As mentioned in the analysis, the pressure ratio and GG speed will fall as the mass flow is extracted from the stream, as their relationship follows a linear function. This is confirmed by Figure 34, displaying the efficiency trend as a function of the deviation in these parameters.

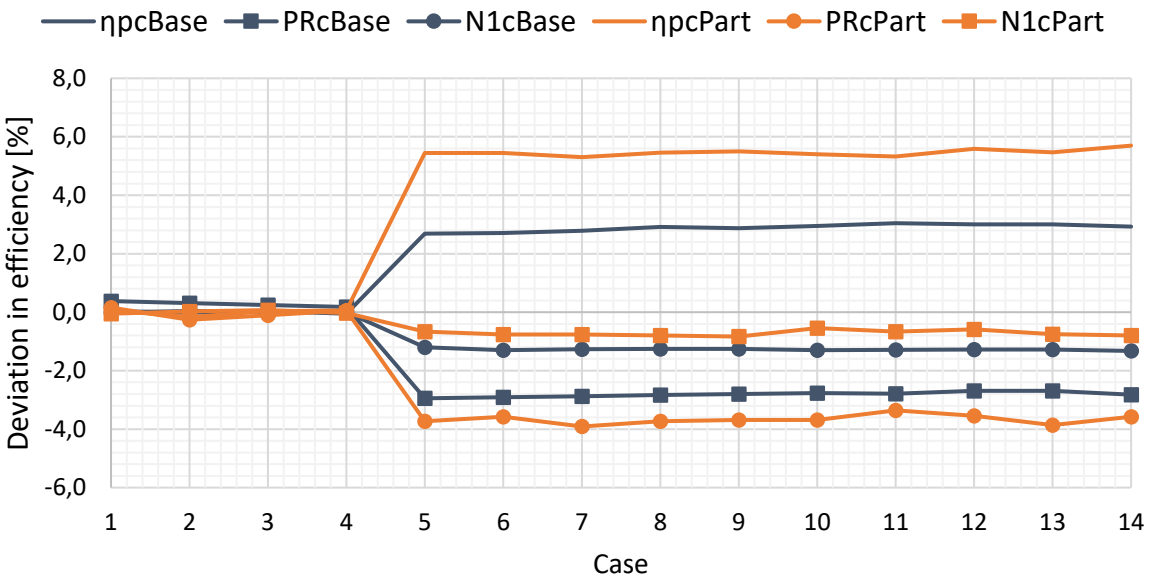

Figure 34: Deviating trends for base and part load compressor polytropic efficiency vs. coinciding operating parameter trends.

Based on this knowledge the factors K_1 and K_2 from Equation 9 correcting for pressure ratio and GG speed respectively can be calculated from Equation 10. This gives the final correction formula for polytropic efficiency at hot bleed anti-ice activation for both base and part load running machines.

$$\eta_{pcorr} = \eta_{pc} \cdot \left(1 + \frac{PR_c - PR_{cref}}{PR_{cref}}\right) \cdot \left(1 + \frac{N_{1c} - N_{1cref}}{N_{1cref}}\right) \tag{11}$$

The results from this correction is displayed below in Figure 35 for both base and part load. Axial magnitudes are kept constant to better emphasize the improvement from Figure 32.

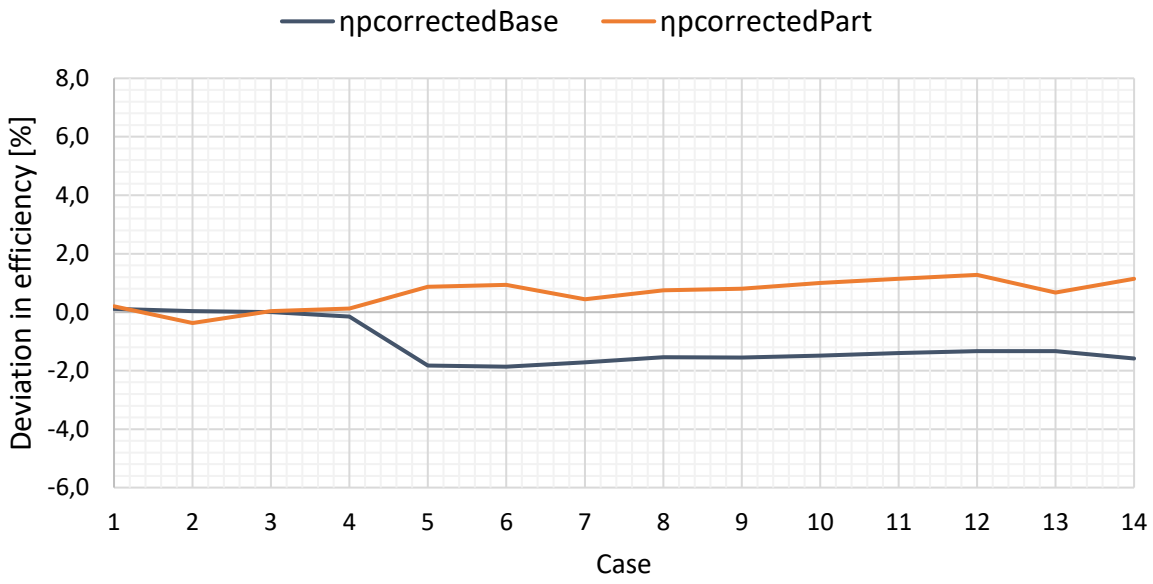

Figure 35: Corrected polytropic efficiency trends for compressor A.

The correction results suggest a relatively passive change due to anti-ice activation of ± 1% (see Figure 35). It is clear that the former deviations have been corrected for, as expected. There is a sudden change in the first cases for the base load trend close to 2%, but it is followed by a steady climb to 1% as the conditions stabilize.

6.2.2 Thermal efficiency

When correcting the thermal efficiency for the extraction of air in the compressor, some things needs to be considered. As the warm air is extracted from the discharge of the compressor, T_{3c} will experience a sudden drop, requiring the combustor to supply more fuel to keep the TIT constant. Therefore, these parameters are investigated closer in Figure 36.

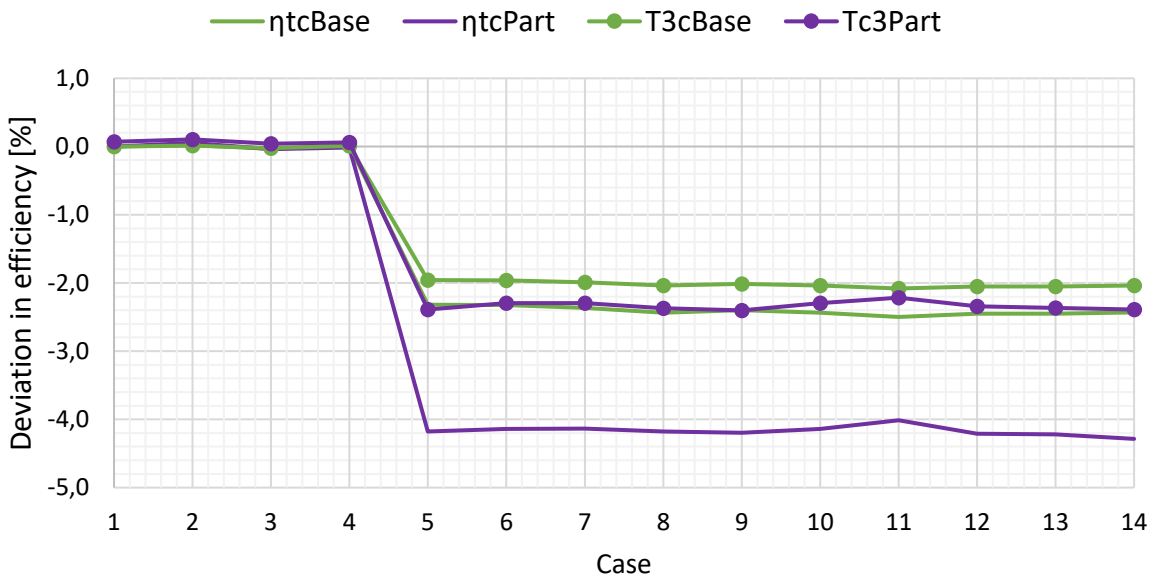

Figure 36: Deviating trends for base and part load thermal efficiency vs. coinciding operating parameter trends.

Based on these findings the correction factor K_1 can be calculated using Equation 10. Utilizing this equation gives the final correction formula for thermal efficiency for both base and part load running gas turbines.

$$\eta_{tcorr} = \eta_{tc} \cdot \left(1 - \frac{T_{3c} - T_{3cref}}{T_{3cref}}\right) \tag{12}$$

Figure 37 is displaying the corrected results following the procedure proposed above. The axial magnitudes are kept constant to emphasize the change in the trends.

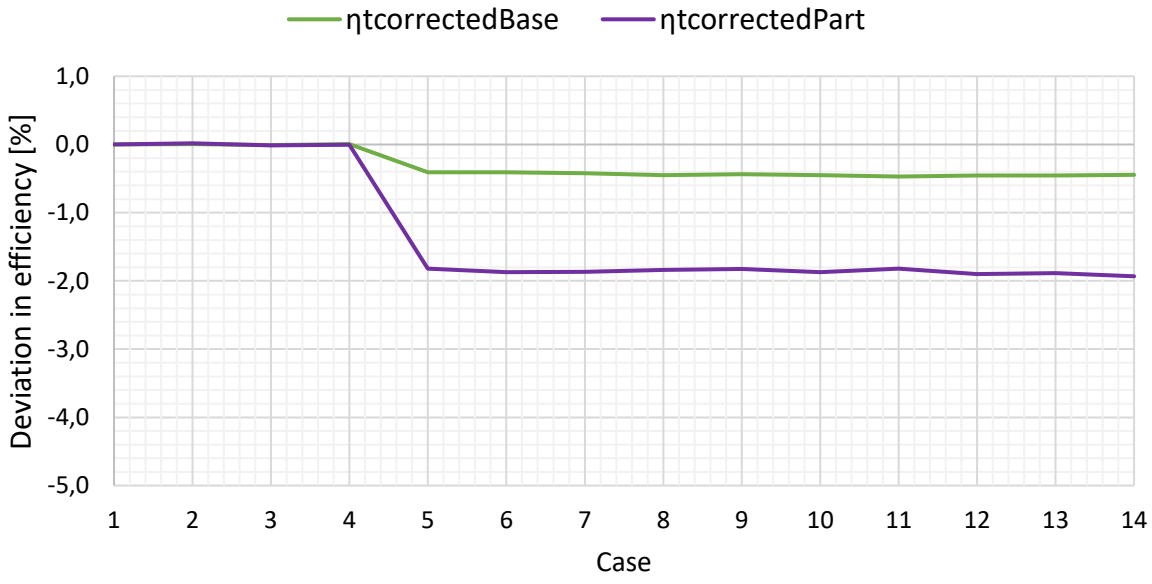

Figure 37: Corrected thermal efficiency trends for compressor A.

The improved thermal efficiency trends are clearly demonstrated in Figure 37. The drop of 2.4% and 4.2% deviation are corrected to 0.4% and 1.8% deviation for base and part load respectively. Now the trends are displaying more correct efficiencies. As the warmer inlet air will eventually decrease the overall efficiencies of the gas turbine slightly, as documented by Hadik [19], some drop is permitted. Taking this fact into consideration, the suggested procedure is promising, as the deviations have been corrected, but there is still work to be done, as discussed in the conclusion.

6.3 Summary, conclusion and further work

As deviating trends in efficiency manifests themselves in the monitoring program offshore, operating and especially diagnosing engines in operation becomes difficult. Therefore, the impact of the anti-ice technology needed to be analysed in order to ascertain the cause of the deviation. The analysis of the anti-ice technology hot bleed system in Chapter 5.2, unearthed a need for an additional procedure for correcting the efficiency of the compressor. Chapter 6 suggests such a procedure.

The analyses of the compressor operational parameters showed the operating point in the map moving away from the BEP due to altering PR_c and N_{1c}. As these parameters are in close relationship with the mass flow according to the compressor map, correction factors were calculated from their reference deviation. The results are promising as they show great ability of correcting of the mass flow extraction effect, decreasing the differences from 3% to -1% and 5.5% to 1% for base and part load, respectively.

The overall thermal efficiency of the gas turbine was discovered to deviate in part by the drop in T_{3c}. This drop causes the control system to increase the fuel flow delivered to the combustor to keep TIT constant. This increase in fuel flow results in a drop in thermal efficiency as the fuel/air flow increase. The results are promising because the deviations are reduced from 2.4% and 4.2% to 0.4% and 1.8% for base and part load, respectively. Some drop is still visible as the inlet temperature to the compressor is heated, affecting density and pressures reducing the thermal efficiency.

Although promising results, further work is still needed. As stated in Chapter 2.4.3, the inclusion of the ISO standard correction exponents for θ and δ factors a and b respectively, can be corrected. Including these exponents has the potential of correcting the parameters further as it takes several conditions otherwise ignored into account. As in previous chapters this chapter's work suffered from lacking important operational parameters such as TIT, mass and

fuel flow as well as other downstream temperature and pressure parameters. A more thorough inspection of the anti-ice systems impact could have been possible with this information. As changes in power output of the gas turbine usually implies changes in the thermal efficiency, power output is interesting. Further work should include considerations on how the power output fluctuates along with power turbine parameters.

7. Thesis summary and conclusion

The objectives of this project have been to present and analyse different anti-ice technologies and how their activation impact the gas turbine operation.

This task commenced by an investigation of the icing phenomenon to better understand the challenges the different inlet systems face. Precipitate and condensate icing are both icing phenomena so diverse and complicated that only a thorough system of inlet heating and filtration working in tandem would suffice.

A literature review of how the ice prevention systems activation and filtration impacts the operation of the gas turbine followed. As the systems prevent icing by injecting warm air into the inlet of the gas turbine all the systems affect the engines thermal efficiency negatively. It is only hot bleed and waste heat recovery that do not recirculate the polluted exhaust gas. In addition, hot bleed extraction from the compressor disrupts the equilibrium between the GG components, and thus reduces the efficiency and the power output from the PT. A consideration of upgrading to a waste heat recovery system, with self-cleaning filters, is recommended. The complexity of additional space and costs need to be a factor in this decision.

This conclusion was verified in the analysis of both the hot bleed and waste heat recovery systems with offshore data. The activation of the two systems prompted changes in the operational parameters which moved both engines' BEP away from the equilibrium line. Relative change of important performance parameters such as GG speed and pressure ratio were of greatest magnitude in the flow extraction system of the hot bleed as expected. This produced the conclusion that the best choice for anti-ice application fell on waste heat recovery. This was further assured by the fact that a waste heat system is reusing the warm exhaust gas, increasing the cycle thermal efficiency vs. the hot bleed which utilizes compressed warm air extracted from the gas turbine flow decreasing thermal efficiency.

Based on the findings in this thesis, the efficiencies of compressor A are making deviations in trend not applicable to theory. Therefore, the task of producing a procedure capable of correcting for the increase or decrease in polytropic or thermal efficiency respectively, was initiated. Since analyses displayed large variations in $N_{1c}$and PR_c, moving the operating point away from BEP, correction factors were established based on their trend deviation. The results show that they are corrected from 3% to -1% and 5.5% to 1% deviation for the base and part load operation respectively. Some deviation in the results is to be expected as the trends stabilize

to a new steady flow. Similarly, the thermal efficiency was corrected for T_{3c} as it dictates the fuel flow to the combustor to keep TIT constant. The procedure corrected the 2.4% and 4.2% to 0.4% and 1.8% for base and part load respectively. Some drop is still visible due to T_2 drop, affecting inlet density and pressures.

A unique and simple correction procedure has been suggested in this thesis. No other procedures, to the author's knowledge, suggests correction factors based on a thorough analysis of two different anti-ice technologies in base and part load. More work is still needed, but the conclusion is that the procedure shows great promise.

8. Further work

Working with analyses of thermal machinery, the measurements of parameters are of prime importance, they are vital to understanding and describing the behaviour of these complicated machines. The quality and quantity of the data available to the author has highlighted some issues that needs attention.

The lack of data on mass flow has been a hampering factor. The measuring of accurate mass flow is extremely difficult, so the power output of the machine could have been given for calculating an approximation. Together with fuel flow, or specific fuel consumption, these factors determine the composition and condition of the exhaust air, and are therefore directly related to turbine power output, heat rate, or thermal efficiency, and waste heat recovery potential. Having these data would make the job of identifying deterioration easier. Further, the pressure and temperature of the inlet of the HPT would have made a thorough inspection possible, instead assumptions had to be made. Data on humidity would be of interest as the amount of water in the inlet air is crucial. Humidity is vital to understanding and predicting operational behaviour and produces a better picture of the weather conditions.

For even more precise and thorough analyses of the engine's performance and the impact of inlet systems the author recommends some notes for further works.

When correcting for inlet conditions and referring them to ISO standards, the inclusion of the θ and δ exponents a and b, respectively, are crucial. Corrections for all the preconditions mentioned in Chapter 2.4.3 is documented to have the potential of more accurate results. As mentioned in previous work, by the author [2], the development of a complete gas turbine simulation model in order to get a more complete picture of the inlet systems impact on operation would be interesting. The additional option of implementing a bleed valve to the discharge flow of the compressor would also support validation of parameters for the entire machine e.g. HPT and PT.

References

1. Volponi, A.J., *Gas turbine parameter corrections.* Journal of engineering for gas turbines and power, 1999. **121**(4): p. 613-621.
2. Aamodt, E., *Gas Turbine Deterioration and Recovery*, in *Department of Energy and Process*. 2018, NTNU: Trondheim.
3. Saravunamuttoo, H., et al., *Gas turbine theory*. 2009, Pearson, Essex, UK.
4. GeneralElectric. *Gas Turbine Power Generation*. 2018 [cited 2018 02. may]; Available from: https://www.ge.com/power/gas/gas-turbines/lm2500.
5. Batcho, P.F., et al., *Interpretation of gas turbine response due to dust ingestion.* Journal of engineering for gas turbines and power, 1987. **109**(3): p. 344-352.
6. Dahl, G.C., *Stall precursor determination of an LM-2500 gas turbine*. 2007, NAVAL POSTGRADUATE SCHOOL MONTEREY CA.
7. Kurzke, J. *Model based gas turbine parameter corrections*. in *ASME Turbo Expo 2003, collocated with the 2003 International Joint Power Generation Conference*. 2003. American Society of Mechanical Engineers.
8. Greitzer, E.M., *Surge and rotating stall in axial flow compressors—Part I: Theoretical compression system model.* Journal of Engineering for Power, 1976. **98**(2): p. 190-198.
9. De Jager, B. *Rotating stall and surge control: A survey*. in *Decision and Control, 1995., Proceedings of the 34th IEEE Conference on*. 1995. IEEE.
10. Leonard, G. and J. Stegmaier, *Development of an aeroderivative gas turbine dry low emissions combustion system.* Journal of Engineering for Gas Turbines and Power, 1994. **116**(3): p. 542-546.
11. Bakken, L. and L. Skogly. *Parametric modelling of exhaust gas emission from natural gas fired gas turbines*. in *ASME 1995 International Gas Turbine and Aeroengine Congress and Exposition*. 1995. American Society of Mechanical Engineers.
12. Regjeringen. *Avgiftssatser*. Skatter og avgifter 2018 12.11.2017 [cited 2018 12.06.2018]; Available from: https://www.regjeringen.no/no/tema/okonomi-og-budsjett/skatter-og-avgifter/avgiftssatser-2018/id2575160/.
13. Administration, E.I., *Natural Gas 1998 - Issues and Trends*. 1999: https://www.eia.gov/oil_gas/natural_gas/analysis_publications/.
14. Brekke, O., L.E. Bakken, and E. Syverud. *Filtration of gas turbine intake air in offshore installations: the gap between test standards and actual operating conditions*. in *ASME Turbo Expo 2009: Power for Land, Sea, and Air*. 2009. American Society of Mechanical Engineers.
15. Maas, D.M. and N.M. McCown. *Turbine Inlet Ice Related Failures and Predicting Inlet Ice Formation*. in *ASME Turbo Expo 2007: Power for Land, Sea, and Air*. 2007. American Society of Mechanical Engineers.
16. Wilcox, M., R. Kurz, and K. Brun. *Successful Selection and Operation of Gas Turbine Inlet Filtration Systems*. in *Proceedings of the 40th Turbomachinery Symposium*. 2011. Texas A&M University. Turbomachinery Laboratories.
17. Loud, R. and A. Slaterpryce, *Gas turbine inlet air treatment.* GE Power Generation, New York, Report No. GER-3419A, 1991.
18. Sammak, M., *Anti-icing in gas turbines*, in *Department of Energy Sciences*. 2006, Lund University. p. 128.
19. El Hadik, A., *The impact of atmospheric conditions on gas turbine performance.* Journal of Engineering for Gas Turbines and Power, 1990. **112**(4): p. 590-596.

20. Dickson, J., *Extreme cold weather operation of gas turbines show key problems. .* Oil and Gas Journal. **74**(17): p. 104-110.
21. Patton, R. *Gas turbine operation in extreme cold climates*. in *ASME 1976 International Gas Turbine and Fluids Engineering Conference*. 1976. American Society of Mechanical Engineers.
22. Mathioudakis, K. and A. Tsalavoutas. *Effects of Anti-Icing System Operation on Gas Turbine Performance and Monitoring*. in *ASME Turbo Expo 2001: Power for Land, Sea, and Air*. 2001. American Society of Mechanical Engineers.
23. Ojo, C.O., et al. *Optimization of Anti-Icing Limits for Alstom Gas Turbines Based On Theory of Ice Formation*. in *ASME Turbo Expo 2009: Power for Land, Sea, and Air*. 2009. American Society of Mechanical Engineers.
24. Matbour, F., H. Alahyari, and F. Namvar, *Anti-Icing System at Gas Turbine Compressor Bell-Mouth and Inlet Guide Vane (IGV).* International Academic Journal of Science and Engineering, 2016. **3**(6): p. 74-82.
25. Øverli, J.M., *Strømningsmaskiner - Termiske Maskiner bind 3*. 2 ed. 1992: Tapir.
26. McKee, R.J. *Mapping and predicting air flows in gas turbine axial compressors*. in *ASME Turbo Expo 2003, collocated with the 2003 International Joint Power Generation Conference*. 2003. American Society of Mechanical Engineers.
27. Røkke, N., J. Hustad, and S. Berg. *Pollutant Emissions From Gas Fired Turbine Engines in Offshore Practice: Measurements and Scaling*. in *ASME 1993 International Gas Turbine and Aeroengine Congress and Exposition*. 1993. American Society of Mechanical Engineers.
28. Samnøy, L., *Gas Turbine Deterioration and Recovery*, in *Department of Energy and Process Engineering*. 2016, NTNU: Trondheim.
29. Schultz, J.M., *The polytropic analysis of centrifugal compressors.* Journal of Engineering for Power, 1962. **84**(1): p. 69-82.
30. Salit, M.L. and G.C. Turk, *A drift correction procedure.* Analytical chemistry, 1998. **70**(15): p. 3184-3190.

Appendices

A: Compressor simulation model in HYSYS

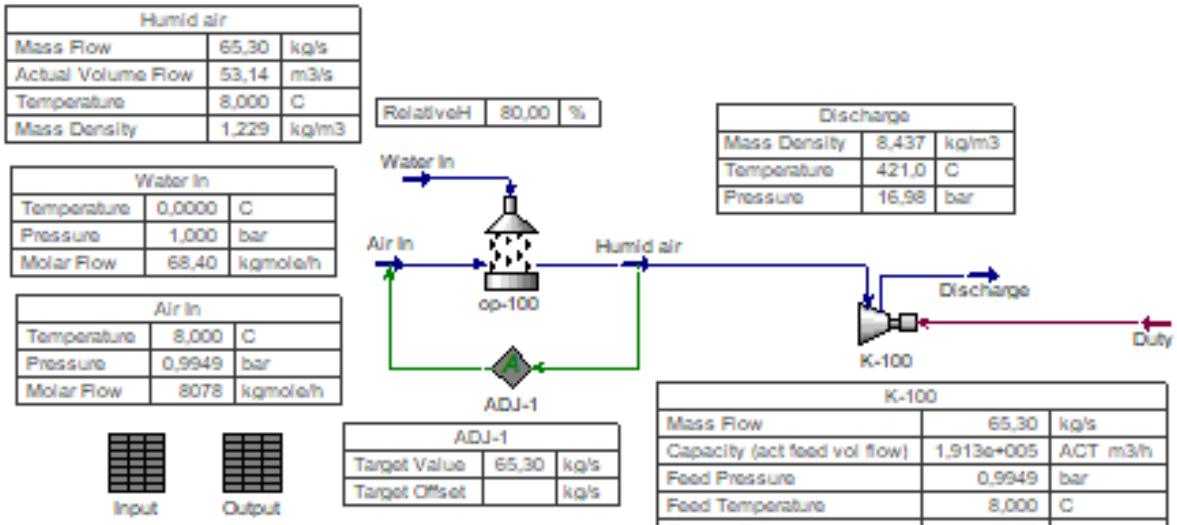

Figure 38: HYSYS compressor simulation model [2].

B: Detailed description of the SRK EOS

The inverse relation between gas volume and pressure where first supported by Robert Boyle and later formulated by Amedeo Avogadro into what we know today as the ideal gas law:

$$PV_m = RT \tag{13}$$

Van der Waals Equation

Improvements on the ideal gas law were made by Johannes D. Van der Waals who argued that intermolecular forces become significant when temperature and pressure increase. Therefore, Van der Waal improved the ideal gas law to incorporate correction to the volume of molecules and their interactions:

$$\left(P + \frac{a}{V_m^2}\right)(V_m - b) = RT \tag{14}$$

Where *a* refers to the degree of reaction of gas molecules, the term $V_m - b$ represents the "free volume" where molecules can move around. *b* is linked to the volume of the gas molecules and their repulsive forces and both *a* and *b* are constant unique to each gas molecule and are independent of pressure and temperature. The equation can be re-arranged to:

$$P = \frac{RT}{V_m - b} - \frac{a}{V_m^2} \tag{15}$$

Which is balanced by the fact that $\frac{RT}{V_m - b}$ describes attraction pushing molecules together alongside *P* and $\frac{a}{V_m^2}$ representing the repulsive forces between molecules.

At higher pressures the repulsive forces prevail over the attractive ones and this equation, which is reasonable at middle pressures, presents inconsistencies. The constants of the equation and the critical parameters are given with:

$$P_c = \frac{a}{27b^2}, T_c = \frac{8a}{27bR}, V_c = 3b \tag{16}$$

For a single component a critical parameter is the highest value the parameter can have where liquid and vapour can coexist. Although, for multicomponent systems the two-phase region can extend beyond the systems critical point.

Redlich-Kwong Equation (MRK)

The Van der Waals equation was modified to improve the equations ability to reproduce fluid parameters at higher temperatures and pressures. The first term in Equation 21 was modified giving:

$$\left(P + \frac{a}{V_m(V_m + b)\sqrt{T}}\right)(V_m - b) = RT \quad (17)$$

This opened for utilizing the equation for pure gases and their mixtures, but also for *NaCl* and $H_2O - CO_2$ fluids.

Soave-Redlich-Kwong (SRK)

The MRK EOS developed Soave-Redlich-Kwong equation made modifications to the correction factor:

$$P = \frac{RT}{V_m - b} - \frac{a}{V_m(V_m - b)} \quad (18)$$

Using the same equation as MRK, Soave made some adjustments to the *a* factor:

$$a = 0{,}42748\frac{R^2T_c^2}{P_c}[f(T)]^2 \quad (19)$$

The function of the reduced temperature T_r and the acentric factor ω where incorporated into the equation:

$$f(T) = 1 + k\left(1 - \frac{T}{T_c}\right) \quad (20)$$

$$k = 0{,}480 + 1{,}57\omega - 0{,}176\omega^2 \quad (21)$$

Accounting for the molecules without a spherical form the acentric factor is introduced. The molecules without spherical form have $\omega = 0$. K.S. Pitzer introduced it and is calculated by:

$$\omega = -\log_{10}\left(\frac{P_{sat}}{P_c}\right)_{T_r=0{,}7} - 1 \quad (22)$$

Soave did not alter the volume correction factor *b*, and maintained it as:

$$b = 0{,}08664\frac{RT_c}{P_c} \quad (23)$$

The modification done in SRK presented a marked impact on calculations of hydrocarbons and the biggest advancements upon which later EOS where built. This includes among others Peng-Robinson (PR) an EOS very similar to SRK but are slightly altered to focus more on petroleum systems, especially gas/condensate systems [19].

C: Details on the implementations of Schultz real-gas relations

Schults' method proposed a simple iterative way of accounting for real-gas relations in the calculations, which is given below:

I. Note inlet η, $T_i$and P_i. Calculate V_i with $k = \frac{c_p}{c_v}$.

II. Estimate outlet temperature T_o:

$$T_o = T_i \left(\frac{P_o}{P_i}\right)^{\frac{k-1}{k}} \tag{24}$$

III. Estimate average pressure $\bar{P}$:

$$\bar{P} = P_i \sqrt{\frac{P_o}{P_i}} \; or \; \bar{P} = \frac{P_o + P_i}{2} \tag{25}$$

IV. Estimate average temperature $\bar{T}$:

$$\bar{T} = \frac{T_o + T_i}{2} \tag{26}$$

V. Estimate average heat capacity ratio $\bar{k}$:

$$\bar{k} = \frac{k_i + 2k_{\bar{T},\bar{P}} + k_o}{4} \tag{27}$$

VI. Estimate compressibility function $\bar{X}$:

$$\bar{X} = \frac{T}{V}\left(\frac{\delta V}{\delta T}\right)_P - 1 \; at \; \bar{P}, \bar{T} \tag{28}$$

VII. Estimate compressibility function $\bar{Y}$:

$$\bar{Y} = \frac{T}{V}\left(\frac{\delta V}{\delta P}\right)_T - 1 \; at \; \bar{P}, \bar{T} \tag{29}$$

VIII. Estimate polytropic temperature exponent $\bar{m}$:

$$\bar{m} = \frac{\left(\frac{\bar{k}-1}{\bar{k}}\right)\left(\frac{1}{\eta} + \bar{X}\right)\bar{Y}}{(1+\bar{X})^2} \tag{30}$$

IX. Estimate polytropic volume exponent $\bar{n}$:

$$\bar{n} = \frac{(1+\bar{X})}{Y\left[\frac{1}{\bar{k}}\left(\frac{1}{\eta} + \bar{X}\right) - \left(\frac{1}{\eta} - 1\right)\right]} \tag{31}$$

X. Estimate new outlet temperature T_o:

$$T_o = T_i \left(\frac{P_o}{P_i}\right)^{\bar{m}} \tag{32}$$

XI. Estimate outlet volume V_o:

$$V_o = V_i \left(\frac{P_o}{P_i}\right)^{-\frac{1}{\bar{n}}} \tag{33}$$

XII. Verify n from EOS:

$$\bar{n} = \frac{\ln\left(\frac{P_o}{P_i}\right)}{\ln\left(\frac{V_i}{V_o}\right)} \tag{34}$$

XIII. Compare n-values and adjust T_o estimates or subdivide steps and return to step IV.

XIV. Estimate work W:

$$W \approx \frac{1}{\eta}\left(\frac{\bar{n}}{\bar{n}-1}\right)\frac{Z_i R T_i}{MW}\left[\left(\frac{P_o}{P_i}\right)^{\frac{\bar{n}-1}{\bar{n}}} - 1\right] \approx \frac{f}{\eta}\left(\frac{\bar{n}}{\bar{n}-1}\right)\frac{Z_i R T_i}{MW}(Z_o T_o - Z_i T_i) \tag{35}$$

D: Ambient conditions for gas turbine A

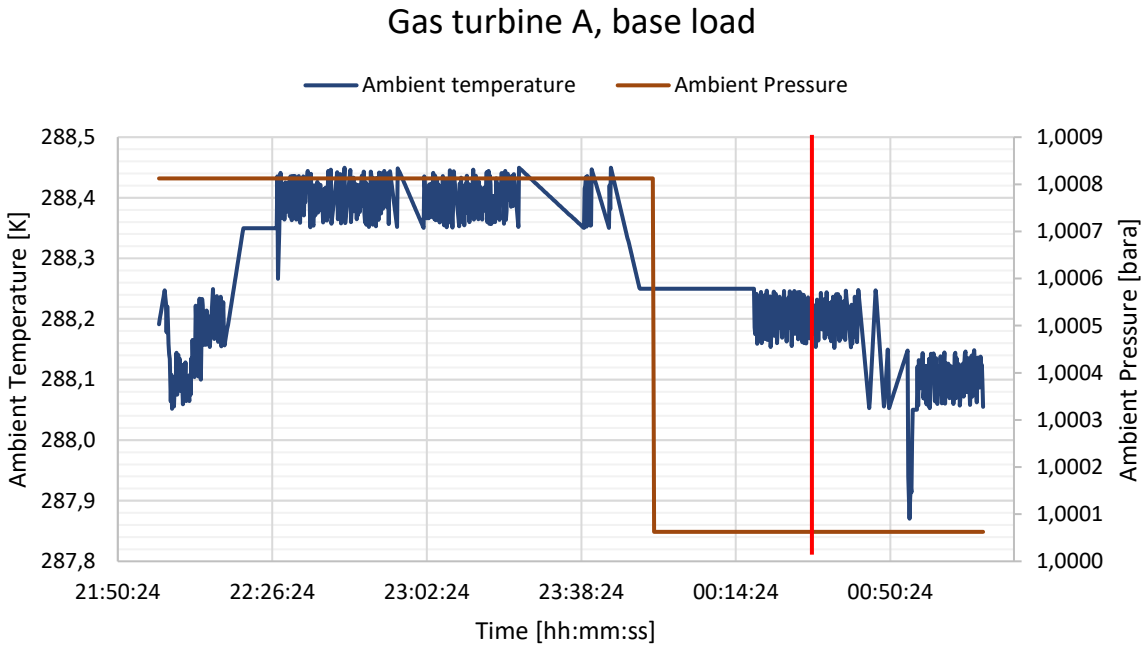

Figure 39: Display of ambient conditions before and after hot bleed anti-ice activation (red line), engine A base. load.

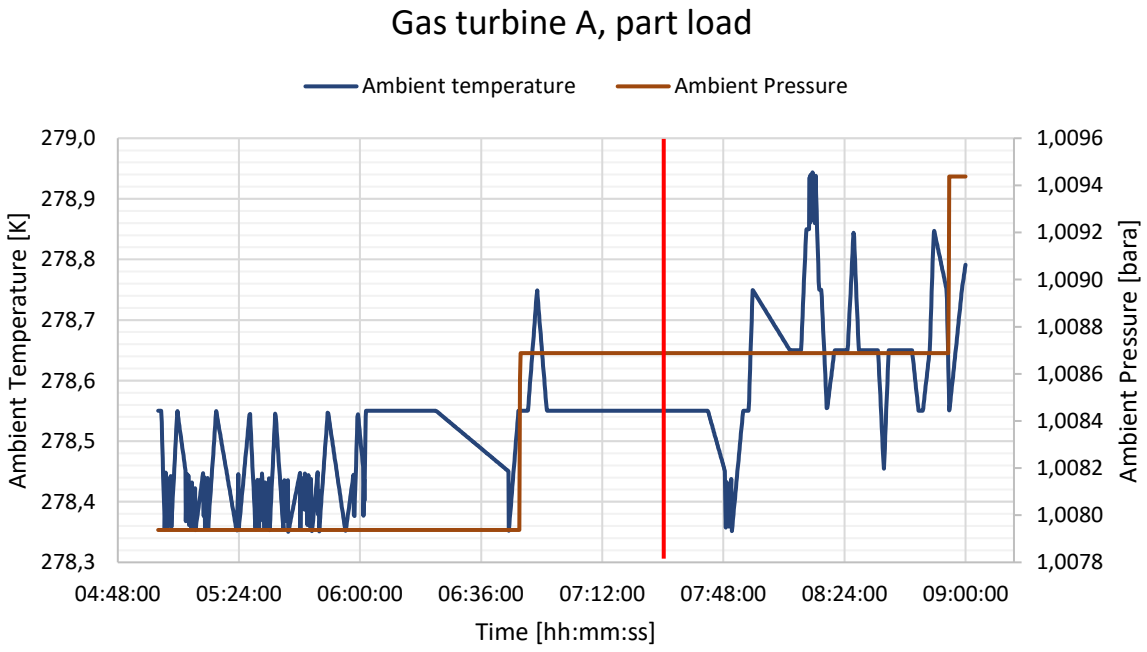

Figure 40: Display of ambient conditions before and after hot bleed anti-ice activation (red line), engine A part load.

E: Ambient conditions for gas turbine B

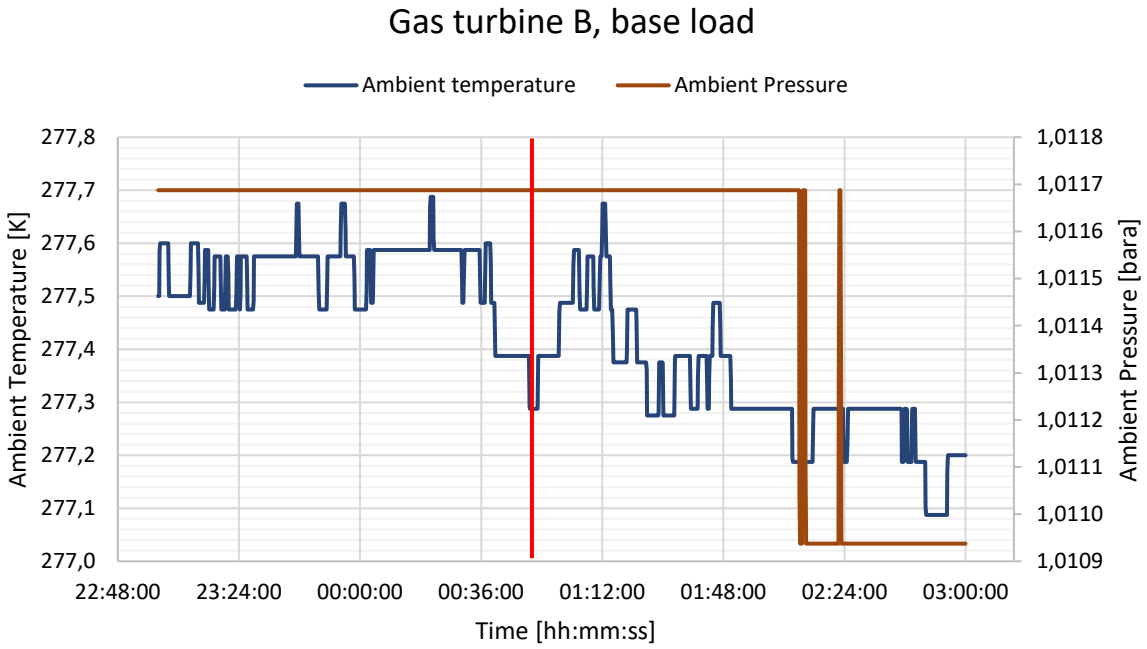

Figure 41: Display of ambient conditions before and after waste heat anti-ice activation (red line), engine B base load.

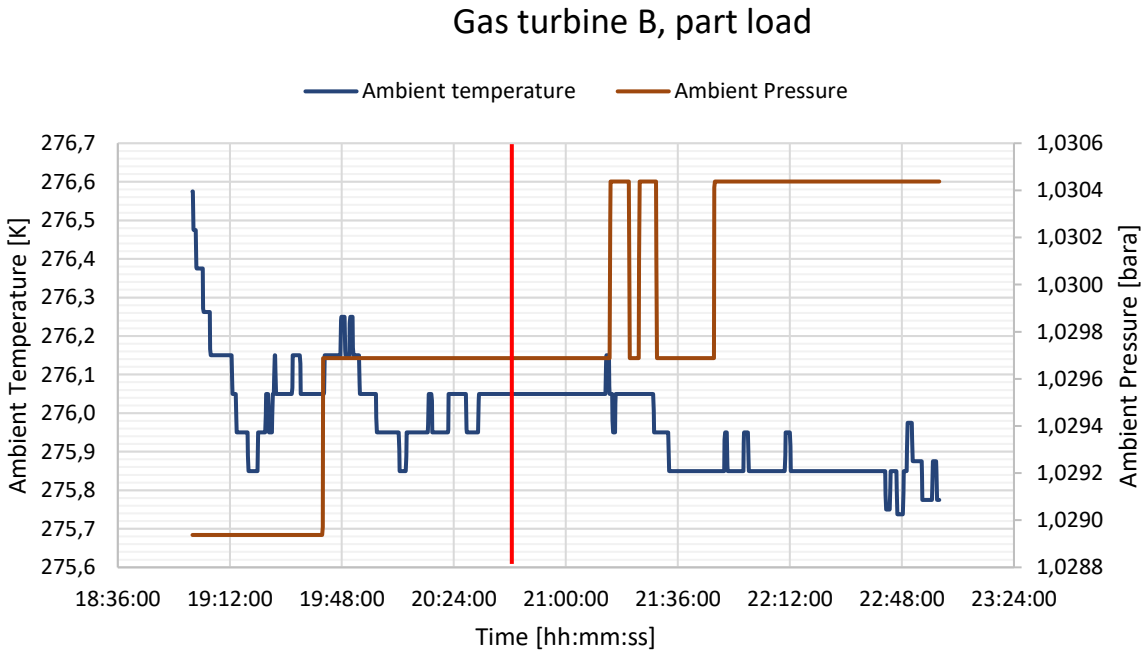

Figure 42: Display of ambient conditions before and after waste heat anti-ice activation (red line), engine B part load.